BNL-20171

NG-316

SURVEY OF PARTIAL-WAVE ANALYSES ON THREE-MESON SYSTEMS(*)

S.U. Chung

Brookhaven National Laboratory, Upton, New York 11973

Talk Presented at

IIIrd International Winter Meeting on Fundamental Physics

Sierra Nevada, Spain

February, 1975

* Work performed under the auspices of the Energy Research and Development Administration.

SURVEY OF PARTIAL-WAVE ANALYSES ON THREE-MESON SYSTEMS

S.U. Chung

Brookhaven National Laboratory, Upton, New York 11973

I. INTRODUCTION

The partial-wave analysis (PWA) of a three-particle system within the framework of the isobar model has been a powerful tool for the study of baryon resonances in, for example, the reaction $\pi N \to \pi\pi N$. The first analysis of this kind on a three-meson system was carried out by Ascoli and his coworkers at Illinois. Since then, his analysis and, in particular, his analysis program has been applied successfully to 3π and $K\pi\pi$ systems over a wide energy range in a number of reactions.

The purpose of this review is to give a comprehensive survey of both the mathematical formalism underlying the analysis and the experimental results of the analysis as applied to 3π and $K\pi\pi$ systems. There has been over the years an informative series of summaries on the experimental results by Ascoli[1-3] and others.[4-8] Our main aim here is not so much to give an up-to-date account of the results as to combine the survey with an exposition of relevant theoretical formulas in order to make this a reasonably self-contained review of one of the more fruitful areas of meson-resonance physics.

In Section II we delve in some detail into the full range of mathematical tools that are required to describe production and decay of a three-meson system. As will become clear, the exposition here represents our own independent view. In particular, we present and discuss a complete set of orthonormal functions which are suitable for description of a three-meson system. We give, in addition, our own approach to parametrization of the spin-density matrix which guarantees the positivity and rank conditions as well as parity conservation.

We survey, in Section III, first the results of the PWA on $(3\pi)^{\pm}$ data with emphasis on the current status of the A_1, A_2 and A_3 enhancements, and then discuss the results of a recent analysis on the $(3\pi)^{o}$ data, where a possible Regge recurrence of the ω is seen at mass 1669 MeV. Results of the PWA on the $K\pi\pi$ system derive from three charged states: $K^-\pi^+\pi^-$, $\bar{K}^o\pi^o\pi^-$ and $\bar{K}^o\pi^+\pi^-$. Prominent features found in the $K\pi\pi$ systems are the Q-region, the $K\pi\pi$ decay of the $K^*(1420)$ and the L-region. These and other relevant results are given in Section IV.

We give in Section V our view of the future prospects. We present, with particular care, how the current techniques of the PWA can be improved upon at succeeding levels of sophistication. A summary is given in Section VI.

II. $(3\pi)^+$ FORMALISM

We give here the general mathematical tools required to describe the production and decay of a three-meson system. A similar formalism, first treated by Ascoli, can be found in Brockway's thesis[9] and a recent paper by Hansen, et al.[10] Our approach here is essentially the same, as there cannot be much freedom in the "isobar model" as applied to a three-meson system. However, certain derivations and parametrizations are our own, and the results are not identical in "minutiae."

1. Preliminaries

Let us start our for concreteness by selecting the reaction

$$\begin{aligned} \pi^+ p &\to (3\pi)^+ p \\ &\to \pi^+\pi^+\pi^- \end{aligned} \qquad \text{(II.1)}$$

for exposition of our formalism. Let w be the effective mass of the 3π system, $R(\alpha\beta\gamma)$ the Euler angles describing the orientation of the 3π system with respect to a coordinate system fixed in the production process (the precise definition will come later), and θ^* the scattering angle between the initial and final nucleons in the CM. Then the phase-space factor assumes the form, neglecting factors which depend only on w,

$$d\phi_4 \propto d\cos\theta^* \; dw \; dR \; d\phi_3 \qquad \text{(II.2)}$$

where $d\phi_3$ is the Dalitz-plot phase-space element given by (again neglecting explicit dependence on w)

$$d\phi_3 \propto dE_i \; dE_j \qquad \text{(II.3a)}$$

$$\propto ds_i \; ds_j \qquad \text{(II.3b)}$$

$$\propto p_i q_i \; dw_i \; d\cos\theta_i \qquad \text{(II.3c)}$$

where p_i and E_i are the momentum and energy of the particle i in the 3π rest frame (RF)$^+$ and w_i (s_i) is the 2π effective mass (squared) defined cyclically:

$$s_i = w_i^2 = (E_j+E_k)^2 - (\vec{p}_j+\vec{p}_k)^2$$

($\pi-\theta_i$) is the angle between the particles i and j in the (j+k) RF and q_i is the magnitude of the momentum of j in the same RF.

If we denote by T the Lorentz-invariant transition amplitude for process (1), the differential cross-sections assume the form,

$$\frac{d\sigma}{d\cos\theta^* \, dw \, dR \, d\phi_3} \propto \Sigma|T|^2 \qquad \text{(II.4)}$$

where the summation is over the initial and final nucleons and all the factors which depend solely on w and on the overall CM energy have been suppressed.

2. Orthonormal Functions

We shall henceforth consider only a small region of phase space with a given w, $\cos\theta^*$ (or equivalently t, the four-momentum transfer squared between the initial and final nucleon) for the reaction (1) with a definite CM energy. Then the problem of 3π analysis involves 5 independent parameters, $R = (\alpha,\beta,\gamma)$ and $\phi_3 = (E_i,E_j)$. Our task here is to develop a complete set of orthonormal functions which span the entire 5-dimensional space.

For the purpose, let us first introduce two variables which describe the Dalitz plot: one is the angle θ_i defined in (3), and the other is defined via

$$\sin(\tau_i/2) = q_i/q_o, \; q_o = \max(q_i). \qquad \text{(II.5)}$$

Note that τ_i by definition ranges between o and π inclusive, and the value of $o(\pi)$ corresponds to the minimum (maximum) value of q_i, which in turn corresponds to the maximum (minimum) for p_i. Hence, the boundary of the Dalitz plot has been relegated to the values of θ_i and τ_i at o and π. We shall find it convenient to recast $d\phi_3$ in terms of τ_i and θ_i in the following way, again neglecting factors which depend only on w;

$$d\phi_3 \propto \xi(\tau_i) \, dr_i \qquad \text{(II.6a)}$$

$$\xi(\tau_i) = \frac{p_i}{w_i \cos(\tau_i/2)} > 0 \qquad \text{(II.6b)}$$

$$dr_i = \sin\tau_i \, d\cos\tau_i \, d\cos\theta_i. \qquad \text{(II.6c)}$$

Note here that the "phase-space factor" is carried by $\sin\tau_i$ in the sense that dr_i goes to zero when τ_i is equal to o or π. Therefore, the factor $\xi(\tau_i)$ is merely a correction factor (which is always greater than zero) connecting the phase-space element $d\phi_3$ to dr_i which is mathematically more advantageous for our purposes. From now on, we shall drop the subscript i from τ, θ and r; it should be understood that these quantities are defined in one particular 2π rest system which is obtained from the 3π rest system via a pure time-like Lorentz transformation.

We have thus reduced the 5-dimensional space of a 3π system to mathematically simple variables $R = (\alpha\beta\gamma)$ and $r = (\tau\theta)$ with the variables ranging between o to π for β, τ, and θ, and o to 2π for α and γ. We may also define a normalized distribution via

$$I(Rr) \propto \frac{d\sigma}{dRdr} \propto \frac{d\sigma}{dRd\phi_3}\,\xi(\tau)$$

$$\propto \Sigma|T|^2\,\xi(\tau) \qquad \text{(II.7a)}$$

so that

$$I(Rr) = \frac{\Sigma|T|^2\,\xi(\tau)}{\int dRdr\;\Sigma|T|^2\,\xi(\tau)} \qquad \text{(II.7b)}$$

We are now ready to introduce a complete set of orthnormal functions which span the Dalitz plot[11]:

$$\phi_{\nu\sigma}(\tau\theta) = 2^{\sigma}\Gamma(\sigma+1)\;\left[(2\sigma+1)\,\frac{(\nu+1)\;\Gamma(\nu-\sigma+1)}{\Gamma(\nu+\sigma+2)}\right]^{1/2}$$

$$\times\, e^{i\sigma\pi/2}(\sin\tau)^{\sigma}\;C_{\nu-\sigma}^{\sigma+1}(\cos\tau)\;P_{\sigma}(\cos\theta) \qquad \text{(II.8a)}$$

where P_σ is the Legendre polynomial and $C_{\nu-\sigma}^{\sigma+1}$ is the Gegenbauer polynomial[12] $(\nu\geq\sigma)$. The functions $\phi_{\nu\sigma}$ are normalized such that

$$\int\phi_{\nu'\sigma'}(\tau\theta)\;\phi^{*}_{\nu\sigma}(\tau\theta)dr = \pi\delta_{\nu\nu'}\delta_{\sigma\sigma'} \qquad \text{(II.8b)}$$

and $$\phi_{oo}(\tau\theta) = 1. \qquad \text{(II.8c)}$$

From the defining formula (8a), it is clear that the index σ carries the meaning of dipion spin; hence, it will in general have some finite cutoff value, beyond which one need not consider in a given experimental data. Note also that the Bose symmetrization is automatically taken into account, if we choose the dipion system to be the one with like charges and consider only even values of spin σ. Note furthermore that near the dipion threshold one has $\sin\tau_i \propto q_i$, so that the factor $(\sin\tau)^\sigma$ in (8a) plays the role of the angular-momentum barrier effect. The Gegenbauer polynomial which depends only on the variable $\cos\tau$ affords no straightforward physical explanation; it simply picks up the remaining Dalitz-plot variable, and in general the index ν ranges from 0 to ∞.

The orthonormal functions which span the 5-dimensional space can now be written as a product of $\phi_{\nu\sigma}(\tau,\theta)$ and $D^{\ell}_{mm'}(\alpha,\beta,\gamma)$ which of course form a complete orthonormal set over the rotation space $R = (\alpha,\beta,\gamma)$. The distribution $I(R,r)$ can be expanded in terms of these functions,

$$I(R,r) = \sum_{LMN} \sum_{I=0}^{\infty} \sum_{K=0}^{I} \frac{(2L+1)}{(2\pi)^3} H(LMNIK) \times D^{L*}_{MN}(R)\, \phi^{*}_{IK}(r) \qquad \text{(II.9a)}$$

The quantities H(LMNIK) are the experimentally measurable moments given by

$$H(LMNIK) = \int dR dr\, D^{L}_{MN}(R)\, \phi_{IK}(r)\, I(Rr) \qquad \text{(II.9b)}$$

with the normalization

$$H(00000) = 1. \qquad \text{(II.9c)}$$

Two special cases of the expansion (9a) are of some practical importance. First, note that, if we integrate over r, we obtain the familiar expansion in the rotation space:

$$I(R) = \int I(Rr)dr$$

$$= \sum_{LMN} \left(\frac{2L+1}{8\pi^2}\right) H(LMN00)\, D^{L*}_{MN}(R) \qquad \text{(II.10a)}$$

Second, by integrating over R, we obtain an expansion appropriate for a Dalitz-plot analysis:

$$I(r) = \int I(Rr)dR$$

$$= \frac{1}{\pi} \sum_{I=0}^{\infty} \sum_{K=0}^{I} H(000IK)\ \phi^{*}_{IK}(r) \qquad \text{(II.10b)}$$

The efficacy of introducing a complete set of orthonormal functions in R and r space is two-fold: First, it affords a straightforward, unbiased way of assessing the goodness of fit; one simply compares the theoretical (or fitted) and experimental H moments and forms a joint χ^2, from which one derives a goodness-of-fit probability. Second, the expansion (9a) demonstrates the richness of information contained in the joint space of R and r; it demonstrates that, as long as the maximum 3π spin in a problem remains finite, one can in principle determine all the parameters in the problem (and in general unique) because the number of independent moments H is infinite (i.e. I goes to ∞, while L remains finite).

3. $(3\pi)^+$ Decay Amplitude

Our next task is to write down the Bose-symmetrized decay amplitude corresponding to the step decay $J^{\eta} \to S^{\eta_S} + \pi^-$, $S^{\eta_S} \to \pi^+ + \pi^-$, where J(S) is the $(3\pi)^+(2\pi)^o$ spin and η and η_S are the corresponding intrinsic parities. And the amplitude is then given explicitly in terms of the variables R and r.

Let us define the body-fixed axes (that is, to the $(3\pi)^+$ system) as shown in Fig. A. To wit, we choose the negative of the π^- direction in the (3π) RF to be the x-axis and the y-axis in the 3π plane, so that the z-axis is along the normal to the 3π plane. The helicity frames for the two separate 2π subsystems have their axes (x_1,z_1,x_2 and z_2) in the direction as shown in Fig. A. The angles θ_1 and θ_2 are defined in $(\pi_3^-\pi_2^+)$ RF and $(\pi_3^-\pi_1^+)$ RF, respectively, while the angles ε_1 and ε_2 are those corresponding to, respectively, $\vec{\pi}_3^- \cdot \vec{\pi}_1^+$ and $\vec{\pi}_3^- \cdot \vec{\pi}_2^+$ in the (3π) RF.

Then, the decay amplitude for a given 3π spin-parity a = {J,η} with step decays via a number of intermediate $(2\pi)^o$ spins s and helicity λ can be written[13]

$$A^a_m \propto \sum_{s\lambda} D^{J*}_{m\lambda}(\Phi_1, \Theta_1, \phi_1)\ d^s_{\lambda o}(\theta_1)\ f^a_{s\lambda}(w_1) + (1 \to 2) \qquad \text{(II.11)}$$

where $f^a_{s\lambda}(w)$ is the helicity amplitude for a given a and s for the $(\pi_3^-\pi_2^+)$ system. The arguments of the first D function, which specify the orientation of the axes z_1 and x_1 in a coordinate system fixed in the production

process, can be re-expressed in terms of $R(\alpha,\beta,\gamma)$ as follows:

$$R(\Phi_1, \Theta_1, \phi_1) = R(\alpha,\beta,\gamma)\ R(-\varepsilon_1,\pi/2,-\pi/2) \equiv RR_1$$
$$R(\Phi_2, \Theta_2, \phi_2) = R(\alpha,\beta,\gamma)\ R(\varepsilon_2,\pi/2,\pi/2) \equiv RR_2 \qquad \text{(II.12)}$$

The next step in our derivation is to re-express $f^a_{s\lambda}$ in terms of the ℓ-s coupling constants:

$$f^a_{s\lambda}(w_i) \propto \sum_{\ell} (\ell os\lambda | J\lambda)\ Q_{\ell s}(w_i)\ G^a_{\ell s} \qquad \text{(II.13)}$$

where $G^a_{\ell s}$ is the ℓ-s coupling constant and $Q_{\ell s}(w_i)$ contains all the "known" mass or momentum dependence such as the Breit-Wigner form for the $(2\pi)^o$ intermediate state or the angular-momentum barrier factors,

$$Q_{\ell s}(w_i) = P_i^{\ell}\left(\frac{w_i}{q_i}\right)^{s+1} e^{i\delta_s(w_i)} \sin\delta_s(w_i) \qquad \text{(II.14a)}$$

with

$$\cot\delta_s(w_i) = (w_s^2 - w_i^2)/(w_s\Gamma_s)$$
$$\Gamma_s = \Gamma_s^o(w_s/w_i)(q_i/q_s)^{2S+1} \qquad \text{(II.14b)}$$

where w_s and Γ_s^o are the mass and width of the $(2\pi)^o$ intermediate state and $q_s = q_i|_{w_i=w_s}$. The factors appearing in (14a) have been fixed by demanding that the Lorentz-invariant amplitude A have the dependence P_i^{ℓ} for $P_i \approx 0$ and q_i^s for $q_i \approx 0$.[14] The energy dependence on Γ_s given above, although fairly common, is not unique; there is as yet no generally accepted form for the Γ_s energy dependence.

We can now recast (11) using (12) and (13):

$$A^a_m \propto \sum_{\ell s} G^a_{\ell s} \sum_{\mu} D^{J*}_{m\mu}(R)\ E^J_{\mu\ell s}(r) \qquad \text{(II.15)}$$

where

$$E^J_{\mu\ell s}(r) = \sum_{\lambda} (\ell os\lambda | J\lambda) \sum_{i=1}^{2} Q_{\ell s}(w_i)\ D^{J*}_{\mu\lambda}(R_i)\ d^s_{\lambda o}(\theta_i) \qquad \text{(II.16)}$$

We may choose the variable r such that $r = r_3 = \{\tau_3, \theta_3\}$ for the (π_1^+, π_2^+) system. In this way, the requirement for Bose symmetrization can be trivially taken into account in the orthonormal expansion, as pointed out in the previous section.

We are now ready to give a precise meaning as to what we mean by an isobar model; it amounts to assuming that the ℓ-s coupling constants $G^a_{\ell s}$ are indeed constant for a given region of w and t. Our "best dynamical knowledge" concerning the 3π decay is then reflected in the term $O_{\ell s}(w_i)$ given in (14a) and (14b).

4. 3π Production Amplitude

In a non-dynamical description of the 3π production process, the most general and economical tool available is that of the generalized spin density matrix, in which the possibility of interference between different 3π spin-parity states is taken into account. However, it is not always easy to parametrize the density matrix whereby all the constraints the density matrix is subject to are satisfied and at the same time the number of parameters is the same as that of the independent unknowns in a density matrix.

Our approach here is not to derive all the relevant formulae but rather to give a brief outline of the major steps involved in the parametrization. We shall first define a complete set of eigenstates of the reflection operator; this enables one to incorporate in a natural way the constraints of parity conservation in the production process. The second step in the parametrization involves the so-called triangular representation of the reflectivity density matrices. For details of the approach given here, the readers are referred to a paper by Chung and Trueman.[15]

Assuming that the reaction AB→RC takes place in the xz plane (which we call the production plane), the reflection operator can be written

$$\Pi_y = \Pi R_y(\pi) = R_y(\pi)\Pi \qquad \text{(II.17)}$$

where Π is the parity operator and $R_y(\pi)$ represents a rotation by π of the system around the y axis (or the production normal). The reflection eigenstates can be written

$$|\varepsilon am\rangle = [|am\rangle - \varepsilon\eta(-)^{J-m}|a-m\rangle]\ \theta(m) \qquad \text{(II.18)}$$

$$\theta(m) = \frac{1}{\sqrt{2}},\ m > 0$$
$$= \frac{1}{2},\ m = 0 \qquad \text{(II.19)}$$
$$= 0,\ m < 0$$

where $a \equiv J^{\eta}$ is the spin-parity of R and ε is the "reflectivity" related to the reflection eigenvalue:

$$\Pi_y |\varepsilon a m\rangle = -\varepsilon(-)^{2J} |\varepsilon a m\rangle \qquad \text{(II.20)}$$

Note that $\Pi_y^{\,2} = (-)^{2J}$, so that $\varepsilon = \pm 1$ for bosons and $\varepsilon = \pm i$ for fermions. The inverse of (18) is given by

$$|a m\rangle = \sum_{\varepsilon} [\,|\varepsilon a m\rangle\ \theta(m) - \eta(-)^{J+m}\ \varepsilon^{*} |\varepsilon a -m\rangle\ \theta(-m)] \qquad \text{(II.21)}$$

In terms of the reflection eigenstates, the production amplitude for R can now be written,

$$\varepsilon T^{a}_{m\varepsilon_f\varepsilon_i} = \langle \varepsilon a m\ \varepsilon_f | T | \varepsilon_i \eta_A \rangle \qquad \text{(II.22)}$$

where $\varepsilon_i(\varepsilon_f)$ refers to the reflectivity of the initial (final) nucleon B(C). Note that for a spin-1/2 particle, the reflectivity eigenvalue exhausts the spin degree of freedom. From parity conservation, it follows that ε_f is a function of ε and ε_i:

$$\varepsilon_f = -\varepsilon(-)^{2J}\ \varepsilon_i \qquad \text{(II.23)}$$

where we assume the beam particle A to be a pseudoscalar ($\eta_A = -1$).

Now the density matrix in terms of the reflection eigenstates can be written, from (22)

$$\varepsilon \rho^{aa'}_{mm'} = \sum_{\varepsilon_i} \varepsilon T^{a}_{m\varepsilon_f\varepsilon_i}\ \varepsilon T^{a'*}_{m'\varepsilon_f\varepsilon_i} \qquad \text{(II.24)}$$

Note that there is no interference between different reflectivity ε because

of (23) and that, furthermore, the summation over ε_i suffices to accommodate the "external" spin degrees of freedom. So the spin-density matrix is broken up into two disjoint submatrices $^{(+)}\rho$ and $^{(-)}\rho$ as a consequence of parity conservation. An additional consequence is that each of the submatrices $^{(\pm)}\rho$ has rank 2, corresponding to the values $\varepsilon_i = \pm i$. We have chosen the sign of ε [see (18)] such that $^{(+)}\rho$ [$^{(-)}\rho$] has contributions only from the natural (unnatural) parity exchange in the peripheral region.

From (18) and (24) one can give a relationship between the reflectivity density matrix $^{\varepsilon}\rho$ and the conventional one:

$$\varepsilon\rho^{aa'}_{mm'} = \tfrac{1}{2}[\rho^{aa'}_{mm'} - \varepsilon\eta'(-)^{J'-m'}\rho^{aa'}_{m-m'}] \; \theta(m)\theta(m') \qquad \text{(II.25)}$$

A parametrization of $^{\varepsilon}\rho$ which covers all the constraints is given by

$$\varepsilon\rho^{aa'}_{mm'} = \sum_{k=1}^{K} \varepsilon V^{a}_{mk} \; \varepsilon V^{a'*}_{m'k} \qquad \text{(II.26)}$$

where K is the rank of $^{\varepsilon}\rho$ (=2 in our case). The $^{\varepsilon}V$'s have the so-called triangular representation, i.e.

$$\begin{aligned} \varepsilon V_{ik} &= 0, \; k > i \\ &= \text{real}, \; k = i \\ &= \text{complex, otherwise} \end{aligned} \qquad \text{(II.27)}$$

where we use the notation i to represent the combination (a,m). Note that the maximum number of independent real elements in $^{\varepsilon}V$ is N^2 where N is the dimension of the matrix $^{\varepsilon}\rho$, corresponding to the case when k ranges from 1 to N; otherwise, the number is smaller than N^2

Let us consider as an example a 3π system with J^{η}'s 0^-, $1^{\pm}$, $2^{\pm}$ and $3^{\pm}$. Then, the total number of real parameters for $^{(+)}\rho$ [$^{(-)}\rho$] is 16x16 [15x15]. If, however, the rank of $^{\varepsilon}\rho$ is 2 (i.e. k=1 or 2), then the number for $^{(+)}\rho$ [$^{(-)}\rho$] drops to 28 [26]. Note that precisely the same number of elements are required for $^{\varepsilon}V$'s.

Owing to the bilinear form of (26), the positivity of $^{\varepsilon}\rho$ is automatically satisfied in the triangular representation, and one is free to vary each element of $^{\varepsilon}V$ independent of one another. Therefore, by

parametrizing $^{\varepsilon}\rho$ in terms of $^{\varepsilon}V$, one has accomplished the task of representing the full allowed space of $^{\varepsilon}\rho$ without resorting to complicated relationships which result from the constraints of positivity and rank conditions.

5. Full Distribution Functions

The overall 3π amplitude has the form,

$$^{\varepsilon}T_{\varepsilon_i\varepsilon_f} = \sum_{am} {}^{\varepsilon}T^{a}_{m\varepsilon_i\varepsilon_f}\ {}^{\varepsilon}A^{a}_{m} \qquad \text{(II.28)}$$

The decay amplitude here is the analog of (15) in the reflectivity basis[16]:

$$^{\varepsilon}A^{a}_{m} \propto \sum_{\ell s} G^{a}_{\ell s} \sum_{\mu} {}^{\varepsilon}D^{a\,*}_{m\mu}(r)\ E^{J}_{\mu\ell s}(r) \qquad \text{(II.29)}$$

where $$^{\varepsilon}D^{a\,*}_{m\mu}(R) = [D^{J}_{m\mu}(R) - \varepsilon\eta(-)^{J-m} D^{J}_{-m\mu}(R)]\ \theta(m) \qquad \text{(II.30)}$$

And the distribution function can now be written

$$I(Rr) \propto \sum_{\varepsilon\varepsilon_i} |{}^{\varepsilon}T_{\varepsilon_i\varepsilon_f}|^2\ \xi(\tau)$$

so that

$$I(Rr) \propto \sum {}^{\varepsilon}\rho^{aa'}_{mm'}\ {}^{\varepsilon}D^{a\,*}_{m\mu}(R)\ {}^{\varepsilon}D^{a'}_{m',\mu'}(R)$$
$$\times\ G^{a}_{\ell s}\ G^{a'}_{\ell' s'}\ E^{J}_{\mu\ell s}(r)\ E^{J',*}_{\mu'\ell' s'}(r)\ \xi(\tau) \qquad \text{(II.31)}$$

where the summation extends over all the repeated indices. This distribution, however, is not the most general one. It is possible that the production process can influence the waves (ℓ,s), in which case the density-matrix elements should be enlarged:

$$^{\varepsilon}\rho^{aa'}_{mm'}\ G^{a}_{\ell s}\ G^{a'\,*}_{\ell' s'} \rightarrow\ {}^{\varepsilon}\rho(^{a\ell sm}_{a'\ell' s'm'}) \qquad \text{(II.32)}$$

For simplicity, however, we will continue to assume in most cases that the m dependence "factorizes" from that of the waves (ℓ,s).

It is instructive to write down explicitly the probability for a given state $\{a,\varepsilon\}$, i.e. from (31),

$$\varepsilon F^a \propto \sum_m {}^{\varepsilon}\rho^{aa}_{mm} \sum_{\substack{\ell s \\ \ell' s'}} G^a_{\ell s}\, G^{a*}_{\ell' s'}\, e^J_{\ell s \ell' s'} \tag{II.33}$$

where $$e^J_{\ell s \ell' s'} = \sum_\mu \int dr\; E^J_{\mu \ell s}(r)\; E^{J*}_{\mu \ell' s'}(r)\; \xi(\tau) \tag{II.34}$$

This shows that the interference between different waves (ℓ,s) cannot in general be separated, and therefore even the 3π mass spectrum w will in general be influenced by this interference effect.

A few words regarding normalizations are in order at this point. Let us denote the normalized functions by the tildas. Then,

$$\tilde{E}^J_{\mu \ell s}(r) = E^J_{\mu \ell s}(r)/[e^J_{\ell s \ell s}]^{1/2} \tag{II.35}$$

Note that the normalized function is now unitless. Correspondingly, we have, from (34),

$$\begin{aligned} &\tilde{e}^J_{\ell s \ell' s'} = 1, \text{ if } (\ell,s) = (\ell',s') \\ &|\tilde{e}^J_{\ell s \ell' s'}| \leq 1, \text{ if } (\ell,s) \neq (\ell',s') \end{aligned} \tag{II.36}$$

so that the latter may be regarded as a correlation coefficient for the $(\ell s)x(\ell' s')$ interference effect. Let F_o be the quantity proportional to the number of events in a given bin of w and t, i.e. from (33)

$$F_o \propto \sum_{\varepsilon a} {}^{\varepsilon}F^a,$$

or, for the general case of (32),

$$F_o = \sum_{\substack{\varepsilon a m \\ \ell s \ell' s'}} {}^{\varepsilon}\rho\left(^{a\ell sm}_{a\ell' s' m}\right) \tilde{e}^J_{\ell s \ell' s'} \tag{II.37}$$

Then, the most general normalized distribution function is given by

$$I(Rr) = \frac{1}{F_o} \Sigma^{\varepsilon}\rho\left(\begin{smallmatrix} a\ell sm \\ a'\ell's'm' \end{smallmatrix}\right) {}^{\varepsilon}D^{a*}_{m\mu}(R)\ {}^{\varepsilon}D^{a'}_{m'\mu'}(R) \times \tilde{E}^{J}_{\mu\ell s}(r)\ \tilde{E}^{J'}_{\mu'\ell's'}(r)\ \xi(\tau) \tag{II.38}$$

Note that the unknowns are collected in the "super-density matrix" of (32) and that the normalization factor F_o is also a function of the super-density matrix. Of course, the super-density matrix can also be given by the triangular representation:

$${}^{\varepsilon}\rho\left(\begin{smallmatrix} a\ell sm \\ a'\ell's'm' \end{smallmatrix}\right) = \sum_k {}^{\varepsilon}V^{a\ell s}_{mk}\ {}^{\varepsilon}V^{a'\ell's'*}_{m'k} \tag{II.39}$$

With this, the distribution function now has a simple "amplitude representation", i.e.

$$I(Rr) = \frac{1}{F_o} \sum_k \left|{}^{\varepsilon}B_k(Rr)\right|^2 \xi(\tau) \tag{II.40}$$

where

$${}^{\varepsilon}B_k(Rr) = \sum_{\substack{a\ell s \\ m\mu}} {}^{\varepsilon}V^{a\ell s}_{mk}\ {}^{\varepsilon}D^{a}_{m\mu}(R)\ \tilde{E}^{J}_{\mu\ell s}(r) \tag{II.41}$$

Under the factorization assumption, the V's break up into the simpler V's introduced earlier and the decay parameter G's. Thus, in this case,

$${}^{\varepsilon}B_k(Rr) = \sum_{am\mu} {}^{\varepsilon}V^{a}_{mk}\ {}^{\varepsilon}D^{a}_{m\mu}(R) \sum_{\ell s} G^{a}_{\ell s}\ \tilde{E}^{J}_{\mu\ell s}(r) \tag{II.42}$$

We recommend that the formula (40) be used in actual computer programs because of its simple form and resulting ease of handling many indices.

It is instructive to find out the total number of parameters in (38) and see by how much it can be reduced with additional assumptions. Let us take as a concrete example a 3π system with J^{η}'s up to $3^{\pm}$ allowed. All possible states $(a\ell s)$ for s up to 2 are listed in Tables I, II, and III.

The most general case is that corresponding to the super-density matrix of (38): the number N of independent parameters is, from Table III, N = 72x72 + 60x60 = 8,784. This undoubtedly is an impossibly large number! If we restrict the rank of the super-matrix to 2, i.e. k = 1 or 2 in (39), then we have N = 71x4 + 59x4 = 520. If we assume factorization, i.e. the dependence of m is independent of that of (ℓ,s) for each a, we obtain, from Tables I and II, N = 16x16 + 15x15 + 42 = 523; with the rank condition, N = 15x4 + 14x4 + 42 = 158.

A remarkable aspect of the $(3\pi)^{\pm}$ system is that the actual number of waves required to describe the system is considerably less than the maximum. In fact, for w up to 2 GeV, only 10 partial waves, listed in Table IV, are required to describe the bulk of the $(3\pi)^{\pm}$ data. With factorization and rank condition, the number N of independent parameters is merely 26. Given that the potential number of parameters is astronomically large, what one obtains from the $(3\pi)^{\pm}$ analysis is not so much a unique solution but rather a solution with a fair description of the data for a minimum possible set of parameters.

6. Maximum Likelihood Analysis

In this section we list a few relevant comments which might be helpful in a likelihood fit to the (3π) data.

The likelihood method can be applied in two different ways. In a conventional approach, one forms a likelihood function starting from a normalized distribution (38):

$$\mathcal{L}' = \sum_{i=1}^{N_t} \ell n\, I(R_i r_i)$$
$$= \sum_{i=1}^{N_t} \ell n\, F(R_i r_i) - N_t \ell n F_o \qquad \text{(II.43)}$$

where $I(Rr) \equiv F(Rr)/F_o$ and N_t is the number of events in the sample being analyzed. There is no absolute scale in the problem in this approach, for multiplying F and F_o by an arbitrary constant does not affect the likelihood function $\mathcal{L}'$. Therefore, it is necessary to fix F_o to a given number, e.g. N_t. This amounts to keeping the trace of the super-density matrix to a fixed number, which can easily be done as given, for example, in Chung and Trueman.[15] However, one disadvantage is that the dependence of I(Rr) on the actual parameters being varied is quite complicated, which could lead to an inefficient use of the maximum-likelihood program.

A better approach is to use the extended maximum-likelihood method,[10] as was done by Ascoli. In this approach, the likelihood function is

$$\mathcal{L} = \sum_{i=1}^{N_t} \ln F(R_i r_i) - F_o \qquad \text{(II.44)}$$

We now have an absolute scale in the problem, and the maximum-likelihood solution will automatically adjust itself so that $F_o \simeq N_t$. Note that this procedure requires one additional parameter than the previous approach, corresponding to the absence of the trace condition. However, a distinct advantage is that $F(Rr)$ and F_o are now quadratic in the unknowns [see (39)]. It has been stated that the extended maximum likelihood method of (44) is better statistically, for it takes into account the Poisson distribution of the total number of events N_t in the sample. However, any sample of events large enough to give a reliable set of parameters in the analysis should be large enough to make the error on N_t inconsequential.

A possible complication in the analysis might arise when the $(3\pi)^{\pm}$ system has reflections from N^*'s or Δ's. One of the simplest ways of eliminating these reflections is to impose cuts on the experimental data. In this case, the normalization constant F_o is no longer given by (37), but rather

$$F_o = \int_{\text{cut}} dRdr\, F(Rr) \qquad \text{(II.45)}$$

which should replace F_o in (43) and (44), and the integration is over the region outside the cuts.

III. PARTIAL WAVES IN 3π SYSTEMS

1. Results on $(3\pi)^{\pm}$ Data

Since the first publication in 1970 by Ascoli et al.[17] on the partial-wave analysis of a $(3\pi)^-$ system, similar analyses by the same group as well as others have been extended for the $\pi^{\pm}p$ data from 5 GeV/c to 40 GeV/c. And the range of the 3π mass w covered in the analysis goes from the threshold up to 2.1 GeV.

The data on the $(3\pi)^-$ system, obtained from the reaction

$$\pi^- p \to \pi^+\pi^-\pi^- p, \qquad \text{(III.1)}$$

consist of the Illinois data[17] with P_{Lab} at 5 and 7.5 GeV/c, the Illinois world compilation[18] with P_{Lab} ranging from 11 to 25 GeV/c, and the Serpukhov data[19] at 25 and 40 GeV/c. Results on the $(3\pi)^+$ system, from the reaction

$$\pi^+ p \to \pi^+\pi^+\pi^- p, \qquad \text{(III.2)}$$

have so far been reported by three groups on three separate data: the Purdue data[20] at 13 GeV/c, the Aachen/Berlin/Bonn/CERN/Heidelberg (ABBCH) collaboration data[21] at 8, 16 and 23 GeV/c, and the Berkeley data at 7 GeV/c.[22]

In addition, similar analyses have been performed on the coherent dissociation $\pi^- \to (3\pi)^-$ in two different reactions. One of these, an experiment carried out by an Illinois group,[23] involved detection of a 4.33 MeV γ-ray from the excited carbon state in the reaction

$$\pi^- C \to \pi^+\pi^-\pi^- C^* \qquad \text{(III.3)}$$

at P_{Lab} = 6 GeV/c. The other involved a more conventional coherent dissociation on nuclear targets,

$$\pi^- A \to \pi^+\pi^-\pi^- A, \qquad \text{(III.4)}$$

at 22.5 GeV/c, an experiment performed by the Carnegie-Mellon/Northwestern/Rochester group.[24] A summary of these data, together with certain pertinent characteristics, is listed in Table V.

All the aforementioned analyses use the Illinois partial-wave analysis (PWA) program, except the Berkeley work. The formulas used in the Illinois PWA program are not substantially different from those in the preceding section. The differences in the Illinois program are: (1) the 3π analyzer (body-fixed z-axis) is taken to be a vector in the 3π plane, instead of the normal to the 3π plane as in our case; (2) certain minor energy-dependent factors in $Q_{\ell s}(w_i)$ are different; (3) the parametrization of the spin-density matrix is different. These differences are clearly technical in nature; there should not be any substantial difference in the results whichever formulas are used in the analysis. Parameters for the intermediate states ε, ρ^o and f, used in the Illinois program, are given in Table VI. Note that the ε width is large ($\sim$ 400 MeV); the ε state is used in the analysis not so much for its "purported existence" as for its usefulness as a means of parametrizing a large s-wave in the $\pi\pi$ scattering amplitude.

The Berkeley program parametrizes the 3π production amplitude in terms of amplitudes rather than a density matrix. The Berkeley group in fact made one crucial assumption: spin coherence of all the waves considered. In our language, this amounts to setting the rank of ε_ρ to one. In addition, the assumption is made that ε is equal to +1, i.e. no unnatural-parity exchange contribution to the 3π states. This is not a drastic assumption, for it has been known from the results of the Illinois PWA program that $\varepsilon = +1$ is dominant over $\varepsilon = -1$.

Before we go into the actual survey of the results, we shall describe our notations which specify completely a given $(3\pi)^{\pm}$ partial-wave state. They are

$$\begin{array}{ll} & J^{\eta}\ \ell s\ m^{\varepsilon} \\ \text{example:} & 2^{+}\ D\rho^{o}\ 1^{+} \end{array} \qquad \text{(III.5)}$$

Thus, the orbital angular momenta are designated S, P, D and F for $\ell = 0$, 1, 2 and 3, while the intermediate states are given the resonance symbols, i.e. ε, ρ^{o}, f and g^{o} for $s = 0$, 1, 2 and 3. The reflectivity ε is given as a superscript on m, following the conventions of previous analyses.

A complete list of all the waves that have been considered for the $(3\pi)^{\pm}$ system with w up to 2 GeV is given in Table IV. Significant waves have been underlined in the table; note that only 10 waves are found to be important in this mass region.[25] Each of the more important partial waves is shown as a function of mass in Figs. 1-5. It is seen that in all cases the significant partial waves belong to unnatural spin-parity series, produced via natural-parity exchange. For both $(3\pi)^{-}$ and $(3\pi)^{+}$ systems there appear three enhancements, the so-called A_1 ($\sim$1.15 GeV), A_2 ($\sim$1.32 GeV) and A_3 ($\sim$1.65 GeV) states, with the A_1 enhancement being by far the largest in intensity. Each of these states is produced primarily in one partial-wave:

$$\begin{array}{ll} A_1; & 1^{+}\ S\rho^{o}\ 0^{+} \\ A_2; & 2^{+}\ D\rho^{o}\ 1^{+} \\ A_3; & 2^{-}\ Sf\ \ 0^{+} \end{array} \qquad \text{(III.6)}$$

The figures demonstrate, furthermore, that there is little intrinsic difference in the intensities between the $(3\pi)^{+}$ and $(3\pi)^{-}$ systems.

Turning now to a discussion of the resonance phases, all the analyses agree that the A_1 phase variations with respect to other waves are

constant throughout the resonance region; see Figs. 6, 7 and 8. It is clear that a simple resonance interpretation for the A_1 is impossible. A portion of the A_1 bump might indeed be the sought-after $I^G = 1^-$ $J^n = 1^+$ resonance (required from the point of view of the quark model); however, one has to invent a mechanism by which the resonance phase does not vary rapidly relative to the background phase. This is not impossible, as in the model by Bowler,[26] although one does get the feeling that his model is rather contrived. For the time being, one should remember that the Reggeized Deck model of Ascoli and Jones[27] does give the correct phase variation in the A_1 region as well as certain qualitative features of the partial-wave mass spectra. Basically, the model involves on-mass-shell $\pi\pi$ and πN scattering amplitude connected by a Reggeized pion propagator, and the amplitude is symmetrized in the two identical π mesons (see Fig. B). As we shall see later, this Reggeized Deck amplitude is required to understand the relative phase between the A_1 and A_2 as well.

The resonance interpretation of the A_2 bump is secure; all the investigators agree that the phase variation in the A_2 region is as expected from a simple Breit-Wigner form interfering with a relatively constant background phase as shown in Figs. 9, 10 and 11. According to the Serpukhov-data analysis, the mass and width for the A_2^- are (1315 ± 5) MeV and (115 ± 15) MeV, and the Purdue analysis gives for the A_2^+ (1298 ± 7) MeV and (110 ± 23) MeV. The A_2 bump in a sense is an anomaly. This state with $J^n = 2^+$ is the only significant natural spin-parity state in the $(3\pi)^-$ system, and it persists all the way up to $P_{Lab} = 40$ GeV/c, indicating that Pomeron exchange plays an important role in the A_2 production. This idea is further strengthened by observation of the A_2 signal in the coherent process $\pi^- \to \pi^+\pi^-\pi^-$ on carbon at 22.5 GeV/c (see Fig. 12).[22]

The $\sigma(A_2)$ vs. P_{Lab} effect is shown more quantitatively in Fig. 13, where it is seen that $\sigma(A_2)$ decreases as $P_{Lab}^{-0.5}$ from 5 to 40 GeV/c, in contrast to other meson productions via quasi-two-body process which decrease much more rapidly in P_{Lab}.[28] According to the Illinois analysis, the energy dependence of $\sigma(A_2)$, $d\sigma/dt$ for the A_2 and, in particular, the phase difference between the A_1 and A_2 can be understood with an A_2 production amplitude with f and $\mathbb{P}$ (Pomeron) exchanges and the aforementioned Reggeized Deck model for the A_1 (see Figs. 13 and 14). It can thus be said that we now have not only a detailed partial-wave knowledge of the $(3\pi)^\pm$ system from the threshold to the A_2 region, but also a semi-quantitative theoretical understanding of the production of the A_1 and the A_2 as well.

Results on the A_3 enhancement are far from clear. In both the π^-p data and the π^+p data, an enhancement is observed in the partial-wave 2^-Sf but not in, for example, $2^-P\rho^\rho$ (see Fig. 15), so it appears that the A_3 is associated with an $f\pi$ threshold effect somewhat similar to the A_1 enhancement in the $\rho\pi$ system. However, the phase variation of the 2^-Sf

wave with respect to others is confusing. As seen in Fig. 16, $2^-Sf - 2^-P\rho^o$ relative phase shows no significant change in the A_3 region for both the π^+p and π^-p data. However, the A_3 phases with respect to all other background waves show little dependence on the 3π mass in the π^-p data, whereas they exhibit a moderate increase through the A_3 region in the π^+p data. What is clearly needed is large-statistics experiments on both the π^+p and π^-p interactions at relatively high energies, preferably to be analyzed by a single experimental group.

2. Results on $(3\pi)^o$ Data

The partial-wave analysis on a neutral 3π system has so far been performed by a single group, based on the reaction,

$$\pi^+p \to (\pi^+\pi^-\pi^o)\ \Delta^{++}(1236), \qquad \text{(III.7)}$$

with the data dervied from the Berkeley Group A experiment on π^+p interactions at 7.1 GeV/c.[29] The data sample analyzed consists of, after the Δ^{++} selection,

$$\begin{aligned} &6800 \text{ events}, \ 0 \leq |t| \leq 0.36 \text{ GeV}^2 \\ &6000 \text{ events}, \ 0.35 \leq |t| \leq 0.80 \text{ GeV}^2. \end{aligned} \qquad \text{(III.8)}$$

Several new dimensions enter into the problem, if a partial-wave analysis is to be performed on reaction (7). First, the symmetry among the pions depends on the total I-spin of the 3π system, so that the I-spin should be explicitly included among the quantum numbers that characterize a given partial wave. Second, the angular dependence of the Δ^{++} decay at the baryon vertex has to be taken into account. Third and most important, additional quantum numbers and variables make the number of unknown parameters prohibitively large.

It is therefore essential to make some simplifying assumptions before a meaningful analysis can be performed. The assumptions they make are: (1) neglect all amplitudes with a helicity flip of 2 units at both the meson and baryon vertices; (2) restrict the partial waves to those with $J \leq 3$, $\ell+s \leq 3$, and $I \leq 2$ plus an additional wave $(3^-F\rho^o)_{I=0}$. With these assumptions, they have performed maximum-likelihood fits on the data using the production amplitudes as parameters.

The results are shown in Figs. 17, 18 and 19. Several remarkable differences are apparent here when compared to the results on the $(3\pi)^\pm$ systems. Unlike the $(3\pi)^\pm$ systems, the unnatural-parity exchange

contribution is large as seen in Fig. 17. In addition, there is little evidence of the A_2 production with natural-parity exchange. This means that the A_2 resonance $[(2^+D\rho^o)_{I=1}$ wave] must be produced mainly by B exchange and not by ρ. Note also that the A_2 phase, as seen in Fig. 19a, shows variation expected for a simple Breit-Wigner form. The mass and width for the A_2^o, according to this analysis, are (1298 $\pm$ 8) MeV and (122 $\pm$ 12) MeV.

Another remarkable aspect of the results is absence of the A_1 and A_3 bumps (see Fig. 19). This lends credence to the idea that the A_1 and A_3 enhancements are <u>mostly</u> the Deck-type threshold enhancements. One should bear in mind, however, that small portions of the A_1 and A_3 bumps in the $(3\pi)^{\pm}$ systems might be genuine resonant states which are somehow suppressed in the $(3\pi)^o$ system.

Figure 18 shows a significant peak near 1.7 GeV for the partial wave $(3^-F\rho)_{I=0}$. This state is likely to be a Regge recurrence of the ω; hence the name $\omega^*(1700)$. The mass and width for this enhancement are found to be

$$\begin{aligned} m(\omega^*) &= (1.669 \pm 0.011)\ \text{GeV} \\ \Gamma(\omega^*) &= (0.173 \pm 0.019)\ \text{GeV}. \end{aligned} \qquad \text{(III.9)}$$

Both the A_2 and ω^* are produced predominantly by unnatural-parity exchange, presumably the B exchange. The ratios R of natural to unnatural exchange cross sections give a quantitative estimate of this effect:

$$\begin{aligned} R(A_2) &= 0.32 \pm 0.05 \\ R(\omega^*) &= 0.14 \pm 0.07. \end{aligned} \qquad \text{(III.10)}$$

In contrast, the background waves, all of which belong to unnatural spin-parity series, are produced entirely by natural-parity exchange.

IV. PARTIAL WAVES IN $K\pi\pi$ SYSTEMS

Partial-wave analyses of $K\pi\pi$ systems have so far lagged behind those of 3π systems, because the $K\pi\pi$ system is inherently more complex and the available data is relatively small. The $(K\pi\pi)^-$ data based on the reaction,

$$K^-p \to (K^-\pi^+\pi^-)p, \qquad \text{(IV.1)}$$

come from four separate experiments. They are: (1) the Aachen/Berlin/CERN/London/Vienna (ABCLV) collaboration[30] with P_{Lab} at 10 and 16 GeV/c; (2) the Serpukhov experiment[31] at 25 and 40 GeV/c; (3) the Rutherford/Ecole Polytechnique (Paris)/Saclay (RPS) collaboration[32] at 14.3 GeV/c; (4) the Ecole Polytechnique (Paris)/Niels Bohr (Copenhagen)/College de France (Paris) collaboration[33] at 3.95 GeV/c. The RPS experiment analyzes, in addition to reaction (1), the complementary reaction,

$$K^- p \to (\bar{K}^o \pi^o \pi^-) p \qquad \text{(IV.2)}$$

from which valuable information on the overall isospin of $(K\pi\pi)$ systems has been obtained. There is, in addition, an analysis performed by a joint group of Aachen/Berlin/CERN/London/Vienna and Athens/Democritus/Liverpool/Vienna (ABCLV-ADLV) collaborations[34] on the neutral $K\pi\pi$ system from the reaction

$$K^- p \to (\bar{K}^o \pi^- \pi^+) n \qquad \text{(IV.3)}$$

at 8, 10 and 16 GeV/c. Summary of these data is given in Table VII.

Unlike 3π's, the isobar models for the $K\pi\pi$ systems require intermediate resonances not only in $\pi\pi$ systems but also in $K\pi$ systems. They are ε, ρ^o and f for the $\pi\pi$ systems and $\kappa(s=0)$, $K^*(890)$ and $K^*(1420)$ (or K^{**}) for the $K\pi$ systems. Parameters for these resonances, as used on the Serpukhov data, are listed in Table VIII. Again, ε and κ are introduced merely as a simple means of parametrizing large s-waves in $\pi\pi$ and $K\pi$ scattering amplitudes.

On the experimental side, a complication arises because K^- and π^- cannot be always distinguished, especially for low $K^-\pi^-\pi^+$ effective masses. Basically, the solution involves throwing out those events for which it is impossible to distinguish a K^- from a π^-; for details, see Refs. 30 and 31. The effect of the cut can easily be taken into account by correcting the normalization integral in the maximum-likelihood fit.

The partial waves that have so far been considered for the $K\pi\pi$ mass w from threshold to 2 GeV are listed in Table IX. The resulting intensity distributions for the waves as a function of w are shown in Figs. 20, 21 and 22. The Q-region ($\sim$1.3 GeV) is seen to be dominated by a 1^+ wave ($m^\varepsilon=0^+$) with the 0^- wave also showing some enhancement in the region. In the higher mass region (see Fig. 22), there is some indication of the $K^*(1420) \to K\pi\pi$ in the 2^+ wave ($m^\varepsilon=1^+$), and in the L-region ($\sim$1.7 GeV) a bump in the 2^- wave ($m^\varepsilon=0^+$). As in the 3π case, the $K\pi\pi$ system up to w = 2 GeV consists predominantly of unnatural spin-parity states produced via natural-parity exchange (see Fig. 23).

A breakdown of the 1^+ state (see Figs. 24 and 25) indicates that in the Q-region the $1^+SK^*0^+$ wave dominates over the $1^+S\rho 0^+$ wave with the corresponding D-wave states being negligible. As was the case with the A_1 region, the phase of the 1^+SK^* wave shows little variation with respect to w in this region (see Fig. 26). Thus, the 1^+SK^* enhancement is again not a simple Breit-Wigner resonance. Furthermore, the Q enhancement seems to be a composite of different spin-parity states; as mentioned earlier, the 0^- wave tends to peak also in the Q-region.

The 2^+ wave shows a small but significant structure in the 1.4 GeV region. This signal, which presumably is due to the $K^*(1420)$ decay, is seen to be composed entirely of the 2^+DK^* and not the $2^+D\rho^0$, as shown in Fig. 27. According to the Serpukhov-data analysis,[31] the $K^*\pi$ to $K\pi$ branching ratio is

$$\frac{K^{*-}(1420) \to (K^*\pi)^-}{K^{*-}(1420) \to (K\pi)^-} = 0.65 \pm 0.13. \qquad \text{(IV.4)}$$

Another way of reliably measuring the branching ratio is to observe the two decay modes in a non-diffractive channel. One such measurement due to Aguilar-Benitez, et al.,[35] obtained from neutral $K^*(1420)$'s off neutron in K^-p interactions, gives 0.47 ± 0.08 for the branching ratio, quite consistent with the result of the partial-wave analysis.

Let us now turn to a discussion of the L-region. Figure 28 shows the partial-wave decomposition of the 2^- wave in the L-region. It appears that the L enhancement comes mostly from the $2^-SK^*(1420)$ wave, analogous to the 2^-Sf dominance in the A_3 region. Due to limited statistics, information on the phase variation on the 2^- state is not yet available. In any case, it seems likely that more than one spin-parity states constitute the L-bump (see Fig. 29), a situation similar to that of the Q-region. One should bear in mind that a sharp K^* enhancement at 1760 MeV has been observed in the reaction $K^-p \to K^-\pi^+n$ and another enhancement at 1710 MeV in the reaction $K^-p \to K^-\omega p$, both observed in the BNL K^-p data at 7.3 GeV/c.[36,37] It seems reasonable to assume that one or both of these enhancements have decay modes into $K\pi\pi$ systems, further complicating the L-region analysis.

Information on the overall isospin of the $K\pi\pi$ system comes from the RPS analysis of reaction (2) at 14.3 GeV/c.[32] By comparing the 1^+SK^* and $1^+S\rho$ waves in the two reactions (1) and (2), they conclude that the $K\pi\pi$ system in the Q-region is mostly I=1/2. The results of separate analysis in reactions (1) and (2) are otherwise similar (see Fig. 20), despite the absence of ε intermediate state in reaction (2).

One remarkable aspect of the RPS analysis concerns the production dependence of the subsystems $K^*\pi$ and $K\rho$ in the Q-region. They find that the waves 1^+SK^* and $1^+S\rho$ have markedly different production dependence (the m dependence). Indeed, the 1^+SK^* wave is produced predominantly in the state $m^\epsilon = 0^+$ in the t-channel reference frame (the t-channel helicity conservation), whereas the $1^+S\rho$ is mainly $m^\epsilon = 0^+$ in the s-channel frame (the s-channel helicity conservation). This suggests that $J^\eta = 1^+$ subsystems $K^*\pi$ and $K\rho$ have different dynamical origins. Note in this regard that the Q-region might harbor two different K^* resonances (C = +1 and C = -1), strange partners to the A_1 (be it Deck or resonance) and the B-meson.

Results on a neutral $K\pi\pi$ system, from the charge-exchange reaction (3), are relatively meager due to a paucity of statistics. What is known about this system, as found by the ABCLV-ADLV collaboration[34] on combined data of 8, 10 and 16 GeV/c, can be summarized as follows. A partial-wave analysis has so far been performed in one mass range $1.04 < w < 1.56$ GeV. They find in this mass range 35% 2^+ state which they attribute to the $K^*(1420)$ decay, 42% 1^+ state and 24% 0^- state. The fraction of unnatural-parity exchange, at about 20%, is somewhat larger than that for the charged $K\pi\pi$ system. The 1^+ state is mostly in the $1^+SK^*0^+$ wave, similar to that in $(K\pi\pi)^-$, but the $m^\epsilon = 1^+$ state seems relatively more important here.

V. POSSIBLE IMPROVEMENTS AND FUTURE PROSPECTS

What improvements can one make on the partial-wave analyses performed so far? What are their future prospects? These questions can be dealt with at several levels. On a more immediate level, one might attempt to reanalyze the A_3 region with both $(3\pi)^+$ and $(3\pi)^-$ data to see if the question of the phase variation can be resolved. However, the existing data may not be sufficient and one might have to wait for much larger statistics with higher P_{Lab} ($\gtrsim$ 40 GeV/c). Similarly, a large-statistics experiment on $K\pi\pi$ systems with high P_{Lab} would be required to do a detailed study of the L(1770) region, including that of the phase variation. For both the 3π and $K\pi\pi$ systems, a wider variety of final states should be studied to gain information on the isospin-dependent structures. They may come, for example, from the reactions: $\pi^+n \to \pi^+\pi^-\pi^0p$, $K^-p \to \pi^+\pi^-\pi^0\Lambda$, $\pi^-p \to (K\pi\pi)^0\Lambda$, $\pi^+n \to (K\pi\pi)^+\Lambda$, etc. In addition, with accumulation of sufficient statistics in the future, one can extend the partial-wave analysis to such final states as $\pi^+\pi^-\eta$, $K\bar{K}\pi$, $\pi^+\pi^-\omega$, etc.

At a technical level, a more systematic measure of the goodness-of-fit has to be employed so as to demonstrate that the best fit indeed gives an acceptable description in the full five-dimensional space. A straightforward way of achieving this goal might be to calculate χ^2's using the moments H(LMNIK), obtained by evaluating the orthonormal functions for

each event. Another approach in this regard involves the experimental $\mathcal{L}$ of (II.44) and its error:

$$\mathcal{L}_{exp} = \sum_{i=1}^{N_t} \mathcal{F}_i, \tag{V.1}$$

$$\delta\mathcal{L}_{exp} = \sum_{i=1}^{N_t} (\mathcal{F}_i)^2, \tag{V.2}$$

where

$$\mathcal{F} = \ell n\ F(R,r) - F_o/N_t \tag{V.3}$$

A theoretical expectation value for $\mathcal{L}$ can be calculated,

$$\mathcal{L}_{th} = N_t \int dRdr\ \mathcal{F}(R,r)\ I(R,r) \tag{V.4}$$

From these, one can form a global "standard deviation,"

$$\sigma(\mathcal{L}) = |\mathcal{L}_{exp} - \mathcal{L}_{th}|/\delta\mathcal{L}_{exp} \tag{V.5}$$

which may be viewed as a measure of the goodness-of-fit.

Another area of further study and improvements concerns the angular-momentum barrier effects. Note that the isobar model as given in Section II calls for the factors $p^\ell q^s$ in an ℓ-s coupling scheme. It is clear that these factors are necessary to avoid kinematical singularities near the thresholds ($p \approx 0$ or $q \approx 0$). However, it is far from certain that these factors prevail in the region far above the thresholds. There are many ways of modifying the simple barrier factors; perhaps the simplest way might be to take the transformation

$$p^\ell \to [p/\sqrt{p^2 + \chi^2}]^\ell \tag{V.6}$$

and similarly for q^s as well. Note that the righthand side approaches p^ℓ as $p \to 0$, while it goes to one as $p \to \infty$. Here the parameter χ can be left as a free parameter in the fit or fixed at some value, say at 0.5 GeV, and one can assess its effect in a resulting fit. An additional improvement of the isobar model could involve inclusion in the fit of the exotic intermediate states, i.e. I=2 $\pi\pi$ and I=3/2 Kπ phase shifts. It is most

likely that the waves with these intermediate states are small in all mass regions, but their interference with other non-exotic waves might turn out to be important.

At a much more ambitious level, the isobar model will have to include rescattering corrections in the final state (see Fig. C). Ascoli and Wyld[38] have already gone to a considerable length in including this effect within the context of a unitarized 3π scattering amplitude. The results are that spin-parity compositions are roughly the same, although the ε to ρ ratio changes. However, what is particularly serious is that the fit becomes significantly worse. Thus, within the framework of the unitarized version of Ascoli and Wyld, the rescattering corrections are too large, and an entirely different approach to the rescattering corrections is called for. The problems relating to three-body unitarization are complex, and there is as yet no clearcut path to the solutions. One way might be to use approximations spelled out in Aaron and Amado.[39] Or, one might use the three-body K-matrix approach of Graves-Morris.[40] In any case, this area of improvements is one which presents a tremendous challenge to theorists and experimentalists alike.

VI. SUMMARY

In Section II we have presented in some detail mathematical tools relevant for study of a three-meson system. We have given, in particular, a complete set of orthonormal functions appropriate for the five-dimensional space of the $\pi^+\pi^+\pi^-$ system and shown how the requirement of the Bose symmetrization can be built into these functions. It has further been shown that $(3\pi)^+$ decay amplitudes can be parametrized, within the context of the isobar model, in terms of the ℓ-s coupling constants $G^a_{\ell s}$ for each given spin-parity state a. The intermediate dipion states needed for this parametrization are then related in a general way to the $\pi\pi$ scattering amplitudes. The factors $Q_{\ell s}(w_i)$, which carry this information as well as the angular-momentum barrier effects, represent our "best knowledge" of the dynamics of sequential decays.

It was shown, in addition, that spin-density matrices, which characterize production of a $(3\pi)^+$ system, are best parametrized in terms of the reflection eigenstates and that its eigenvalues are connected with the naturality of exchanged particles in the peripheral region. The positivity and rank conditions are easily incorporated into the parametrization of ${}^{\varepsilon}\rho$ (ε is the reflectivity) by use of the triangular representation. If the factorization hypothesis does not hold between the production and decay for a given 3π spin-parity state a, then the coupling constants $G^a_{\ell s}$ may themselves depend on the production-dependent parameters m (the z-component of the 3π spin J) and the initial and final nucleon helicities. The prescription for this case is, as has been demonstrated, to combine ${}^{\varepsilon}\rho$ and $G^a_{\ell s}$ into a super-density matrix, in which the indices range over all the variables $\{a\ell sm\}$.

A survey of the results of partial-wave analyses has been given in Sections III and IV. Briefly, it may be recapitulated as follows. Analyses of the $(3\pi)^{\pm}$ systems show three prominent enhancements, each in a particular partial wave: $1^+S\rho 0^+(A_1)$, $2^+D\rho 1^+(A_2)$, and $2^-Sf0^+(A_3)$. Other waves are definitely present, but the number is small; in all, a total of 10 waves produced via natural-parity exchanges are required to give an adequate description of the $(3\pi)^{\pm}$ system from threshold to 2 GeV (see Table IV).

The A_1 wave shows little phase variation with respect to others in the A_1 region, indicating that the A_1 is not a simple Breit-Wigner resonance. In fact, much of the A_1 region can be understood within the context of a Reggeized Deck model. The A_2 enhancement, which shows phase variations of a simple Breit-Wigner resonance, seems to be produced through exchanges of Pomeron and f trajectories. The situation with the A_3 enhancement is less clear; there is as yet no convincing evidence that the A_3 is not a simple Breit-Wigner resonance. Thus, the answers to this and other related questions can come only with a fresh analysis on a much larger statistical sample than has hitherto been available.

A partial-wave analysis of a neutral $(3\pi)^0$ system from the final state $\pi^+\pi^-\pi^0\Delta^{++}$, according to the Berkeley analysis, indicates that the A_1 and A_3 bumps do not seem to be present and the A_2 state $[(2^+D\rho)_{I=1}]$ is seen to have its typical phase variations. A noteworthy result of the analysis is observation of a $(3^-F\rho)_{I=0}$ enhancement with mass at (1669 $\pm$ 11) MeV and width (173 $\pm$ 19) MeV, a likely candidate for the Regge recurrence of the ω.

Partial-wave analysis on $K\pi\pi$ systems is much less extensive due to inherent complexities of $K\pi\pi$ systems and relative lack of statistics. The $K\pi\pi$ system up to 2 GeV consists mainly of unnatural spin-parity states produced via natural-parity exchanges. The Q-region is dominated by the 1^+SK^* state, but the $1^+S\rho$ state, which is also present in the region, shows different m dependence from that of the 1^+SK^* state, suggesting possibly a different dynamical origin for the two states. As in the A_1 region, the phases between the 1^+ and other waves do not vary in the Q-region. Also, the 1^+ wave does not account for all the events of the Q enhancement; it appears that the 0^- wave peaks in the Q-region as well.

Thus, the Q-region seems to be even more complex than the A_1 region. In a sense, this is not surprising, if one considers that there might be in the Q-region two different I=1/2 states, the strange partners of the B meson and the A_1 (or the "non-Deck" portion of it).

There is only one significant natural spin-parity state: the 2^+DK^* wave which peaks near 1420 MeV. It seems likely that this represents the $K^*\pi$ decay mode of the $K^*(1420)$. In the L-region, one sees an

enhancement in the $2^- SK^*(1420)$ wave, but it does not account for all the events of the L enhancement. For both the 2^+ and 2^- waves, little is known about their phase variations, due mainly to lack of statistics.

In Section V we have considered several possible improvements and future prospects. The field of partial-wave analyses is still young, and with the advent of high-statistics equipments such as the BNL Multi-Particle Spectrometer, CERN Omega and SLAC LASS, we can look forward to a rich and fruitful future in this area of meson-resonance physics.

ACKNOWLEDGEMENTS

The author wishes to thank J. Diaz, J. Rubio, M. Aguilar-Benitez and the entire organizing committee of the Conference for their warm hospitality during his stay in Spain. He is indebted to S. Protopopescu and J. Bensinger for their careful reading of the drafts. Finally, he acknowledges N.P. Samios for his continued encouragement and support.

FOOTNOTES AND REFERENCES

1. G. Ascoli, in Experimental Meson Spectroscopy-1972 (EMS-'72), p. 185.

2. G. Ascoli, in Proc. of the XVI Int'l. Conf. on High Energy Physics, Vol. I, p. 3 (1972).

3. G. Ascoli, in Proc. of the XVII Int'l. Conf. on High Energy Physics, p. II-8 (1974).

4. U.E. Kruse, in EMS-'70, p. 359.

5. R. Klanner, in EMS-'72, p. 164.

6. J.D. Hansen, in EMS-'74, p. 173.

7. G. Otter, in Proc. of the XVII Int'l. Conf. on High Energy Physics, p. II-13 (1974).

8. F. Wagner, in Proc. of the XVII Int'l. Conf. on High Energy Physics, p. II-27 (1974); see Section III.

9. D.V. Brockway, Ph.D. thesis (1970), Univ. of Illinois Report No. COO-1195-197.

10. J.D. Hansen, et al., Nucl. Phys. B81, 403 (1974).

11. The functions we use here have been adapted from: H.R. Hicks and P. Winternitz, Phys. Rev. D4, 2339 (1971); H.R. Hicks and P. Winternitz, Phys. Rev. D5, 2877 (1972). Note that our definition of the angles and the normalization of the functions are not the same.

12. See, for example, Handbook of Mathematical Functions, ed. M. Abramowitz and I.A. Stegun, p. 774 ff.

13. This is the familiar amplitude for the step decay $J \to S + \pi$, $S \to \pi + \pi$. For background information on this and other related subjects, see, for example, S.U. Chung, Spin Formalisms, CERN Report No. CERN 71-8, 1971.

14. The factor w_i in (14a) has its origin in the expression for a Lorentz-invariant $\pi\pi$-scattering amplitude in terms of phase shifts. Note that, instead of (14b), one can in fact use the known $\pi\pi$ phase shifts in (14a).

15. S.U. Chung and T.L. Trueman, Phys. Rev. D11, 633 (1975).

16. The problem of expanding an angular distribution in terms of moments in the reflectivity basis has been worked out in Ref. 15; this paper also contains various properties of the D-functions defined in the reflectivity basis.

17. G. Ascoli, et al., Phys. Rev. Lett. 25, 962 (1970).

18. G. Ascoli, et al., Phys. Rev. D7, 669 (1973), and Phys. Rev. Lett. 26, 929 (1971).

19. Yu. M. Antipov, et al., Nucl. Phys. B63, 141 (1973) and 153 (1973).

20. G. Thompson, et al., Phys. Rev. D9, 560 (1974) and Nucl. Phys. B69, 381 (1974).

21. G. Otter, et al., Nucl. Phys. B80, 1 (1974) (Aachen/Berlin/Bonn/CERN/Heidelberg Collaboration).

22. T.A. Lasinski, in EMS-'74, p. 46.

23. G. Ascoli, et al., Phys. Rev. Lett. 31, 795 (1973).

24. U.E. Kruse, et al., Phys. Rev. Lett. 32, 1328 (1974); J.R. Russ, in EMS-'74, p. 237.

25. For completeness, we point out here that not all waves can be determined uniquely in all mass regions. In particular, the two waves $1^+S\rho^o$ and $1^+P\varepsilon$ are virtually indistinguishable from each other for $w < 1.1$ GeV; see B. Weinstein, G. Ascoli, and L.M. Jones, Phys. Rev. D8, 2904 (1973).

26. M.G. Bowler and M.A.V. Game, Oxford University Report (1974).

27. G. Ascoli, et al., Phys. Rev. D9, 1963 (1974) and Phys. Rev. D8, 3894 (1973); L.M. Jones, in EMS-'74, p. 288.

28. G. Ascoli, et al., Phys. Rev. Lett. 33, 610 (1974).

29. F. Wagner, M. Tabak, and G.M. Chew, LBL-3395 (1975).

30. M. Deutschmann, et al., Phys. Lett. 49B, 388 (1974) (Aachen/Berlin/CERN/London/Vienna Collaboration).

31. Yu. M. Antipov, et al., University of Illinois preprint No. COO-1194-290 (1974).

32. S.N. Tovey, et al., Rutherford Laboratory preprint No. RL75-045 (1975) (Rutherford/Ecole Polytechnique/Saclay Collaboration).

33. B. Drevillon, et al., Phys. Lett. 55B, 245 (1975) (Ecole Polytechnique/Niels Bohr/College de France Collaboration).

34. Submitted to EMS-'74 and reported on by Hansen (see Ref. 6). See also Ref. 7.

35. M. Aguilar-Benitez, et al., Phys. Rev. D4, 2583 (1971).

36. M. Aguilar-Benitez, et al., Phys. Rev. Lett. 30, 672 (1973).

37. S.U. Chung, et al., Phys. Lett. 51B, 413 (1974).

38. G. Ascoli and H.W. Wyld, Unitarity States for Three Pions, University of Illinois preprint (1975); G. Ascoli, in EMS-'74, p. 59.

39. R. Aaron and R.D. Amado, Phys. Rev. Lett. 31, 1157 (1973).

40. P.R. Graves-Morris, Nuovo Cimento 54A, 817 (1968); G. Smadja, Resonances that Overlap, LBL-382 (1971).

TABLE I. Allowed ℓ Values

J^η	s=0	s=1	s=2	$N(G^a_{\ell s})$*
0^-	0	1	2	4
1^+	1	0,2	1,3	8
2^-	2	1,3	0,2,4	10
3^+	3	2,4	1,3,5	10
1^-		1	2	2
2^+		2	1,3	4
3^-		3	2,4	4
			Total	42

* Number of independent real parameters in $G^a_{\ell s}$ for each $a = J^\eta$. Note that one $G^a_{\ell s}$ can be set to one for each a without loss of generality.

TABLE II. Allowed m Values

J^η	ε=+1	ε=-1
0^-	0	
1^+	0,1	1
2^-	0,1,2	1,2
3^+	0,1,2,3	1,2,3
1^-	1	0,1
2^+	1,2	0,1,2
3^-	1,2,3	0,1,2,3
Total number	16	15

TABLE III. Number of Allowed Combinations (aℓsm)

J^η	$\epsilon=+1$	$\epsilon=-1$
0^-	3	0
1^+	10	5
2^-	18	12
3^+	24	18
1^-	2	4
2^+	6	9
3^-	9	12
Total	72	60

TABLE IV. Partial Waves for $(3\pi)^{\pm}$ Systems[a]

J^η	$\epsilon\pi$	$\rho\pi$	$f\pi$	m^ϵ
0^-	S	P	D	0^+
1^+	P	S,D	P,F	$0^+,1^\pm$
2^-	D	P,F	S,D	$0^+,\ 1^\pm,2^\pm$
3^+	F	D	P	$0^+,1^\pm$
4^-		F	D	0^+
5^+		G		0^+
6^-		H		0^+
1^-		P	D	$0^-,1^\pm$
2^+		D	P	$0^-,1^+$
3^-		F	D	$0^-,1^\pm,2^\pm,3^\pm$
4^+			F	1^+

a. This table shows the orbital angular momenta for final states $\epsilon\pi$, $\rho\pi$ and $f\pi$; the waves shown underlined are the significant waves found in fits.

TABLE V. Summary of $(3\pi)^{\pm}$ Data

P_{Lab} (GeV/c)	Selections	Number of Events
π^- at 5 and 7.5 (Illinois)[17]	Δ^{++} and Δ^0 out $t' < 0.7$ GeV^2	12,900
π^- at 11-25 (Compiled B.C. data)[18]	Δ^{++} out $t' < 0.7$ GeV^2	15,300
π^- at 25	$0.10 \leq \lvert t \rvert \leq 0.33$ GeV^2	31,400
π^- at 40 (Serpukhov)[19]	$0.04 < \lvert t \rvert < 0.33$ GeV^2	52,200
π^+ at 13 (Purdue)[20]	$\Delta^{++}(p\pi^+_{slow})$ out $t' < 0.5$ GeV^2	5,250
π^+ at 8, 16, 23 (ABBCH)[21]	Δ^{++} out $t' < 0.8$ GeV^2	11,500
π^+ at 7 (Berkeley)[22]	Δ^{++} out $t' < 0.6$ GeV^2	~30,000

TABLE VI. Intermediate States for $(3\pi)^{\pm}$ Systems[a]

Spin (s)	w_s (MeV)	Γ^o_s (MeV)	Symbol
0	765	400	ε
1	765	135	ρ
2	1264	150	f

a. Values quoted here are those used by Ascoli, et al.[18] The Breit-Wigner form, according to formulas (II.14), is

$$Q_{\ell s}(w_i) \propto p_i^{\ell} q_i^{s} / (w_s^2 - w_i^2 - i w_i \Gamma_s)$$

and $$\Gamma_s = \Gamma_s^o (w_s / w_i)(q_i / q_s)^{2s+1}$$

where w_i is a neutral dipion mass with q_i its breakup momentum, and p_i is the breakup momentum between the dipion and the odd pion in the 3π rest frame. The quantities with subscript s are evaluated with the dipion mass replaced by w_s.

TABLE VII. Summary of $K\pi\pi$ Data

P_{Lab} (GeV/c)	Selections	Number of Events
K^- at 10 and 16 (ABCLV)[30]	Δ^{++} out $t' < 0.8$ GeV^2	4,730[a]
K^- at 40 (Serpukhov)[31]	$0.05<\|t\|<0.60$ GeV^2	10,180[a]
K^- at 14.3 (RPS)[32]	Δ^{++} and Δ^+ out $t' < 0.8$ GeV^2	~19,700[a]
K^- at 3.95 (PCP)[33]	Δ^{++} out $t < 1.0$ GeV^2	1,715

a. In all these data, an additional selection has been made; a fraction of the sample for which a K^- cannot be distinguished from a π^- has been thrown out.

TABLE VIII. Intermediate States for $K\pi\pi$ Systems[a]

Spin (s)	Di-Meson	w_s (MeV)	Γ_s^o (MeV)	Symbol
0	$\pi\pi$	765	400	ε
1	$\pi\pi$	765	135	ρ
2	$\pi\pi$	1269	154	f
0	$K\pi$	1320	600	κ
1	$K\pi$	892	50	$K^*(890)$
2	$K\pi$	1420	110	$K^*(1420)$

a. Quoted values are from the work on the Serpukhov data.[31] See Table VI for definitions of w_s and Γ_s^o.

TABLE IX. Partial Waves for Kππ Systems

J^{η}	ℓs^{a}	m^{ϵ}
0^-	$S\epsilon^{b}$, PK^*, $P\rho$	0^+
1^+	SK^*, $S\rho$, $P\kappa$, $P\epsilon$	$0^+, 1^+$
2^-	PK^*, $P\rho$, $SK^*(1420)$, Sf	0^+
2^+	DK^*, $D\rho$	$1^+, 0^-$
3^+	DK^*, $D\rho$, Pf	0^+

a. Both the orbital angular momenta and di-meson spins are given in their usual notations.

b. $0^-S\epsilon$ and $0^-S\kappa$ are so similar in all variables that they cannot be distinguished experimentally, and the $0^-S\kappa$ is left out of the analysis.

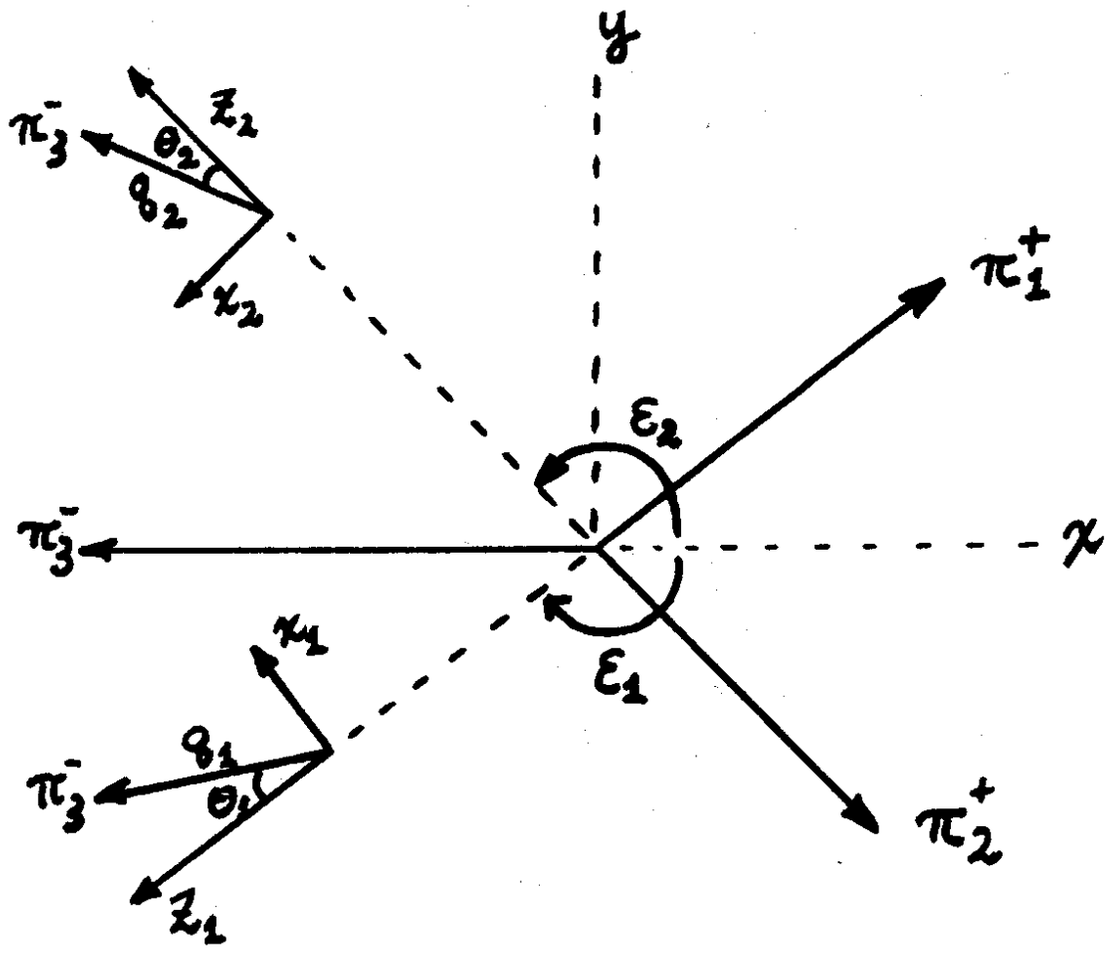

Fig. A. Definition of the body-fixed axes for $\pi_1^+\pi_2^+\pi_3^-$ system; the z-axis is normal to and out of the paper. Also shown are the dipion rest frames for $\pi_2^+\pi_3^-$ (denoted by subscript 1) and $\pi_1^+\pi_3^-$ (denoted by subscript 2).

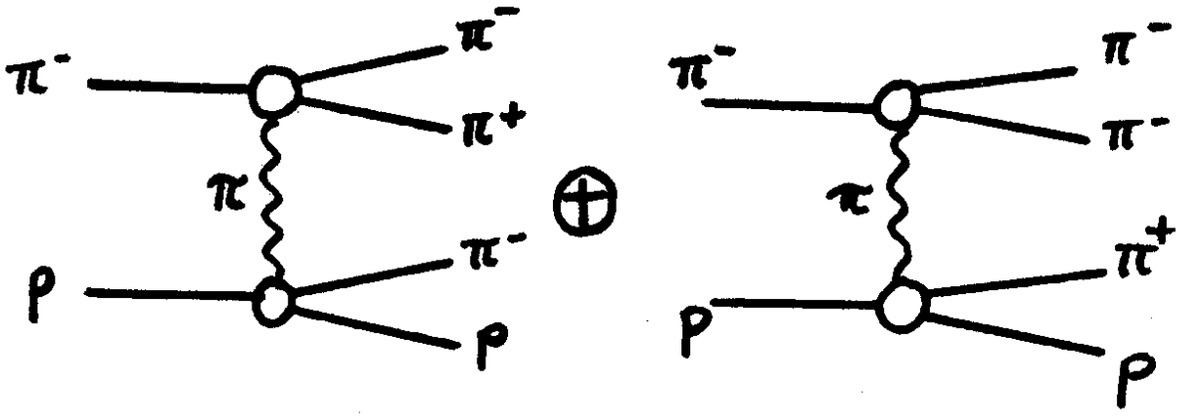

Fig. B. Reggeized Deck model of Ascoli and Jones. The model uses on-mass-shell ππ and πN scattering connected by a Reggeized pion propagator.

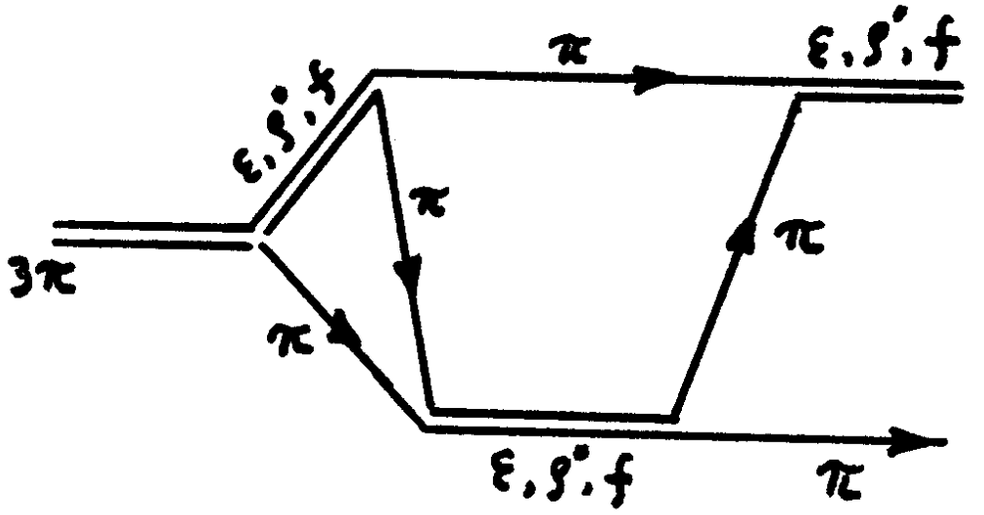

Fig. C. Schematic diagram showing possible rescatterings in the 3π final state.

FIGURE CAPTIONS

1. Partial-wave decomposition for compiled $\pi^- p$ data at 11-25 GeV/c (Ref. 18).

2. Partial-wave decomposition for Serpukhov $\pi^- p$ data at 40 GeV/c (Ref. 19). Notations: $J^\eta \ell m^\varepsilon(s\pi)$ instead of our $J^\eta \ell s m^\varepsilon$.

3. Partial-wave decomposition for Purdue $\pi^+ p$ data at 13 GeV/c (Ref. 20). (Note that intermediate states s have been suppressed in the notations.)

4. Partial-wave decomposition for ABBCH $\pi^+ p$ data at 8, 16 and 23 GeV/c (Ref. 21).

5a[b] Partial-wave decomposition for Berkeley $\pi^+ p$ data at 7 GeV/c with $0 \leq |t| \leq 0.1$ GeV^2 [$0.1 \leq |t| \leq 0.6$ GeV^2] (Ref. 22).

6. Intensity and phase of $1^+S\rho$ wave (Refs. 18 and 19).

7. Phases of $1^+S\rho$ relative to $0^-S\varepsilon$ and $1^+P\varepsilon$ and of $2^+D\rho$ relative to $1^+S\rho$ (Ref. 21).

8. Intensity and phase of $1^+S\rho$ (Ref. 22).

9. Intensity of $2^+D\rho$ and its phases relative to $1^+P\varepsilon$ (upper points) and $1^+S\rho$ (lower points) (Ref. 19).

10. (a) Intensity of $2^+D\rho$ and (b) the Argand diagram for the interference term between $2^+D\rho$ and $1^+S\rho$ (Ref. 20).

11. Intensity and phase of $2^+D\rho$ (Ref. 22).

12. Partial-wave decomposition for $\pi^- \to (3\pi)^-$ on Carbon at 22.5 GeV/c (Ref. 24).

13. (a) σ vs. P_{Lab} for $\pi^- p \to A_2^-(\to \rho^0\pi^-)p$ with $1.2 \leq M(3\pi) \leq 1.4$ GeV and $t' < 0.7$ GeV^2; the solid (dashed) curve is for $K > 0$ ($K < 0$), where K is the ratio of f to $\mathbb{P}$ residues.

    (b) Comparison of the measured to fitted differential cross sections for $\pi^- p \to A_2^-$ ($\to \rho^0\pi^-$)p.

14. Comparison of measured A_2-A_1 interference phase to the phase predicted from Regge and Deck model calculations (Ref. 28).

15. Intensity of 2^-Sf and $2^-P\rho$ from $\pi^+ p$ data, (a) Ref. 18, (b) Ref. 21, (c) Ref. 20, (d) Ref. 19.

FIGURE CAPTIONS (Cont'd.)

16. Phase of 2^-Sf wave relative to $1^+S\rho$, $2^-P\rho$, $0^-S\varepsilon$ and $1^+P\varepsilon$ waves from $\pi^\pm p$ data. ⧓ π^-p(Ref. 18), ⧖ π^-p(Ref. 19), ⧗ π^+p(Ref. 20), ⧓ π^+p(Ref. 21).

17. $\pi^+\pi^-\pi^0$ mass spectrum from the reaction $\pi^+p \to (3\pi)^0\Delta^{++}$ at 7 GeV/c (Ref. 29); the hatched histogram corresponds to the natural-parity exchange cross section.

18. $(3\pi)^0$ mass spectrum (⧓) from $\pi^+p \to (3\pi)^0\Delta^{++}$ for two different t intervals (Ref. 29); the total intensities in the waves $(2^+D\rho)_{I=1}$ (⧖) and $(3^-F\rho)_{I=0}$ (⧗) are also given.

19. (a) Relative phase between $(2^+D\rho)_{I=1}$ and $(2^-Sf)_{I=1}$ for low $|t|$ (Ref. 29).

    (b) Relative phase between natural- and unnatural-parity exchange amplitudes for $(2^+D\rho)_{I=1}$ for low $|t|$; the straight line comes from a Regge model with ρ and B exchanges.

    (c)[d] Total intensity for the $(1^+)_{I=1}$ [$(2^-)_{I=1}$] wave for low $|t|$ (⧗) and for high $|t|$ (⧓).

20. Differential cross sections (in μb/GeV) as a function of $K\pi\pi$ mass for various partial waves from the reaction $K^-p \to K^-\pi^+\pi^-p$ (⧓) and the reaction $K^-p \to \bar{K}^0\pi^0\pi^-p$ (⧓) at 14.3 GeV/c (Ref. 32).

21. Partial-wave decomposition ($J^\eta m^\varepsilon$) for the $(K\pi\pi)^-$ system from $K^-p \to K^-\pi^+\pi^-p$ at 10 and 16 GeV/c (Ref. 30).

22. Partial-wave decomposition ($J^\eta m^\varepsilon$) for $K^-p \to K^-\pi^+\pi^-p$ at 40 GeV/c (Ref. 31).

23. Natural and unnatural spin-parity components for both the produced and exchanged systems (Ref. 30).

24. Decomposition of the 1^+ wave [$J^\eta\ell(s\pi)m$] (Ref. 31).

25. Study of the $K\rho$ and $K^*\pi$ states in the 1^+S state (Ref. 30).

26. Relative phases of the 1^+SK^* wave with respect to other waves (Ref. 31).

27. Intensities of the waves $2^+DK^*1^+$ and $2^+D\rho1^+$ (Ref. 31).

28. Intensities of the waves 2^-Sf, 2^-SK^{**}, $2^-P\rho$ and 2^-PK^* (Ref. 31).

29. Intensities of the waves $1^+S(\rho+K^*)$ and $2^-S(K^{**}+f)$, compared to the $K\pi\pi$ mass spectrum (Ref. 30).

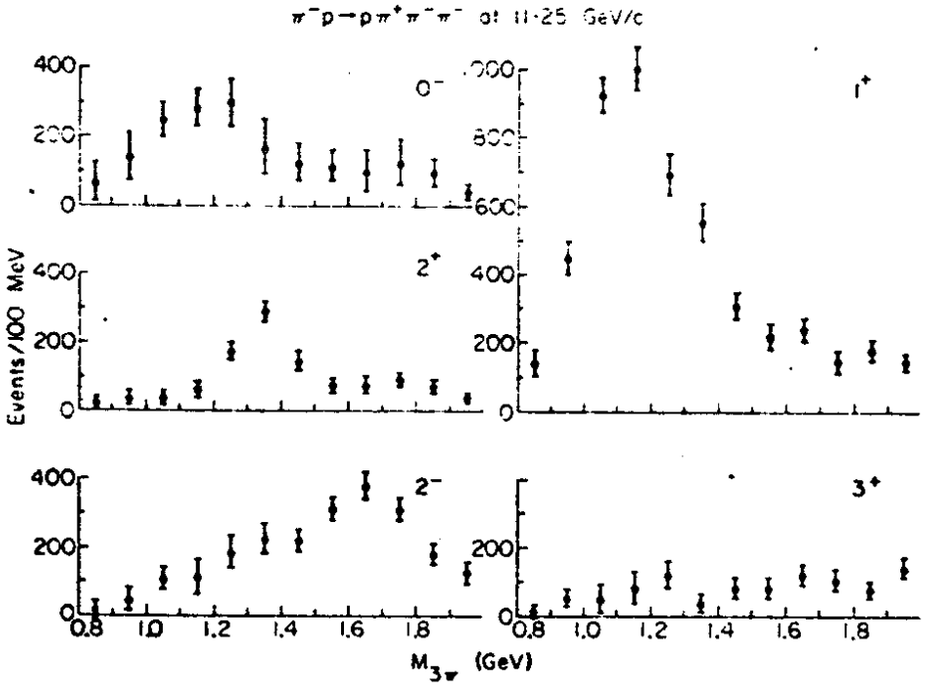

Fig. 1

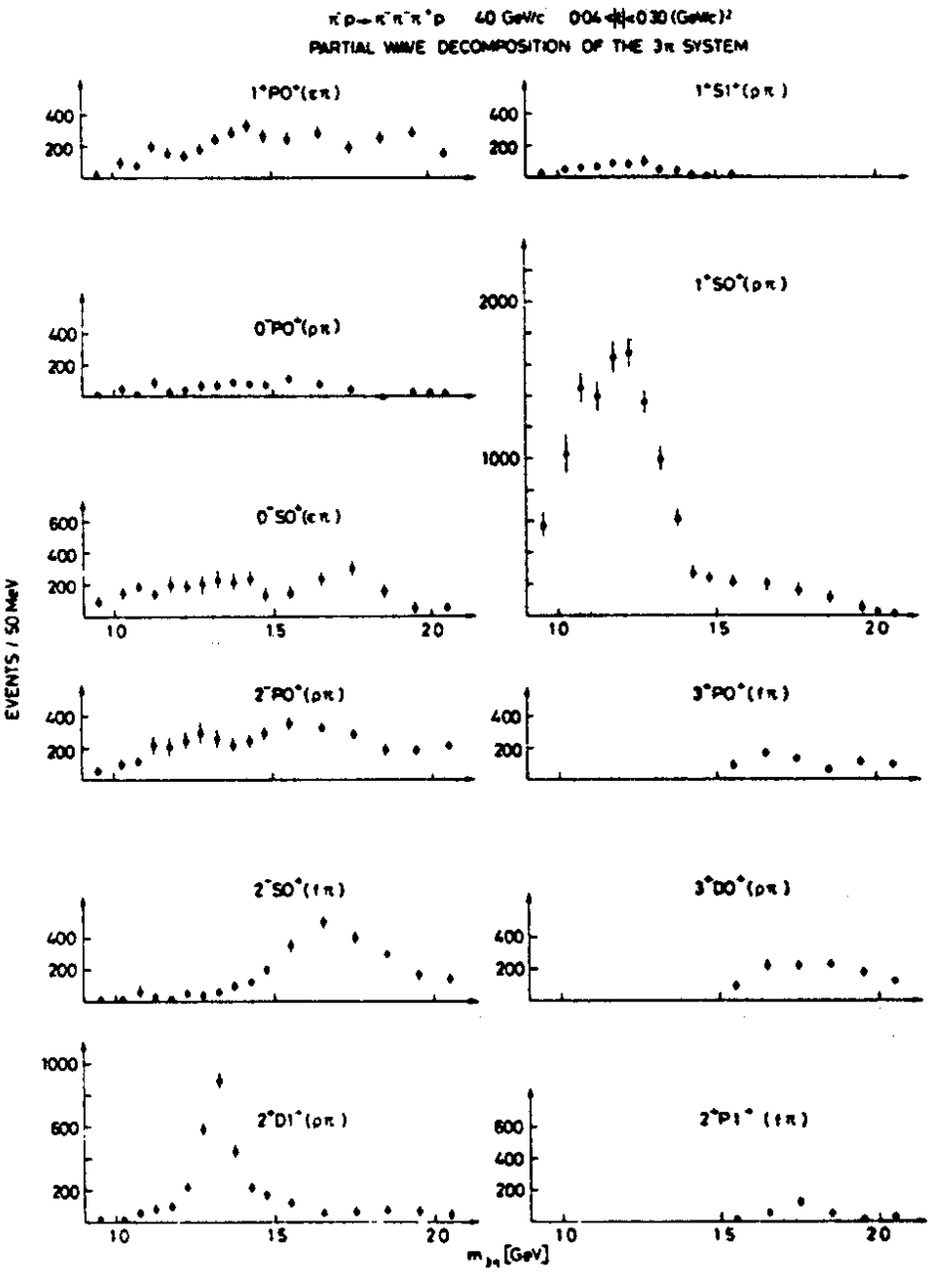
$\pi^- p \to \pi^- \pi^- \pi^+ p$ 40 GeV/c $0.04 < |t| < 0.30$ (GeV/c)^2
PARTIAL WAVE DECOMPOSITION OF THE 3π SYSTEM
$1^+P0^+(\varepsilon\pi)$
$1^+S1^+(\rho\pi)$
$1^+S0^+(\rho\pi)$
$0^-P0^+(\rho\pi)$
$0^-S0^+(\varepsilon\pi)$
$2^-P0^+(\rho\pi)$
$3^+P0^+(f\pi)$
$2^-S0^+(f\pi)$
$3^+D0^+(\rho\pi)$
$2^+D1^+(\rho\pi)$
$2^+P1^+(f\pi)$
EVENTS / 50 MeV
$m_{3\pi}$ [GeV]

Fig. 2

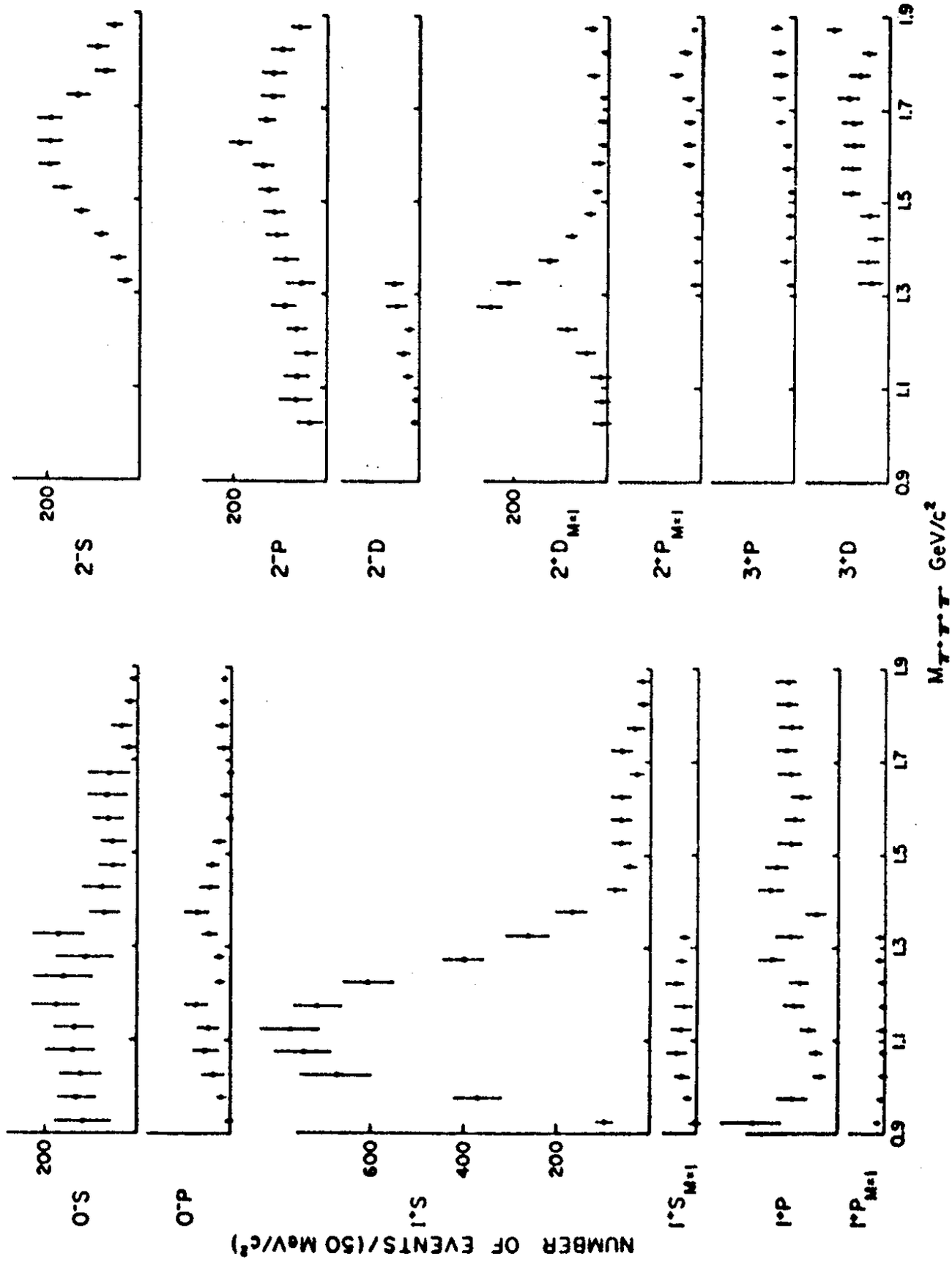
NUMBER OF EVENTS/(50 MeV/c²)
0⁻S
0⁻P
S.I
1⁺S_M=1
1⁺P
1⁺P_M=1
2⁻S
2⁻P
2⁻D
2⁺D_M=1
2⁺P_M=1
3⁺P
3⁺D
200
400
600
0.9
1.1
1.3
1.5
1.7
1.9
M GeV/c²

Fig. 3

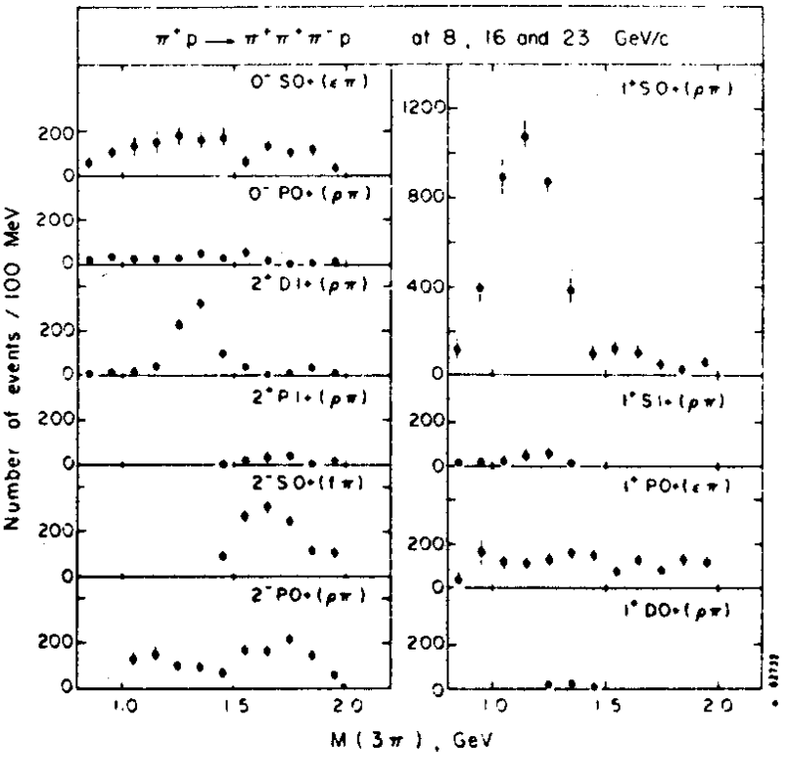
$\pi^+ p \longrightarrow \pi^+\pi^+\pi^- p$ at 8, 16 and 23 GeV/c
$0^- S0^+(\epsilon\pi)$
$0^- P0^+(\rho\pi)$
$2^+ D1^+(\rho\pi)$
$2^+ P1^+(\rho\pi)$
$2^- S0^+(f\pi)$
$2^- P0^+(\rho\pi)$
$1^+ S0^+(\rho\pi)$
$1^+ S1^+(\rho\pi)$
$1^+ P0^+(\epsilon\pi)$
$1^+ D0^+(\rho\pi)$
Number of events / 100 MeV
M (3π) , GeV

Fig. 4

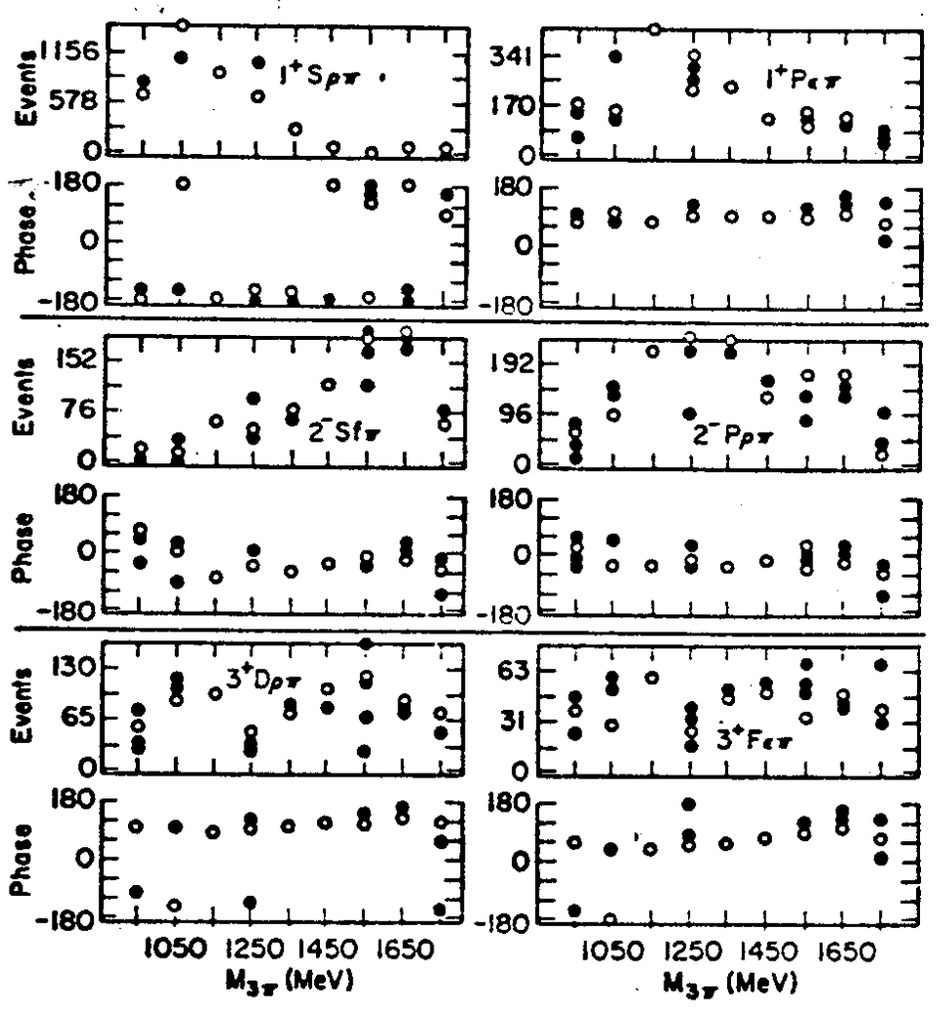
Events
Phase
1156
578
0
341
170
180
-180
152
76
192
96
130
65
63
31
1⁺Sρπ
1⁺Pεπ
2⁻Sfπ
2⁻Ppπ
3⁺Dρπ
3⁺Fεπ
1050 1250 1450 1650
M3π (MeV)

Fig. 5a

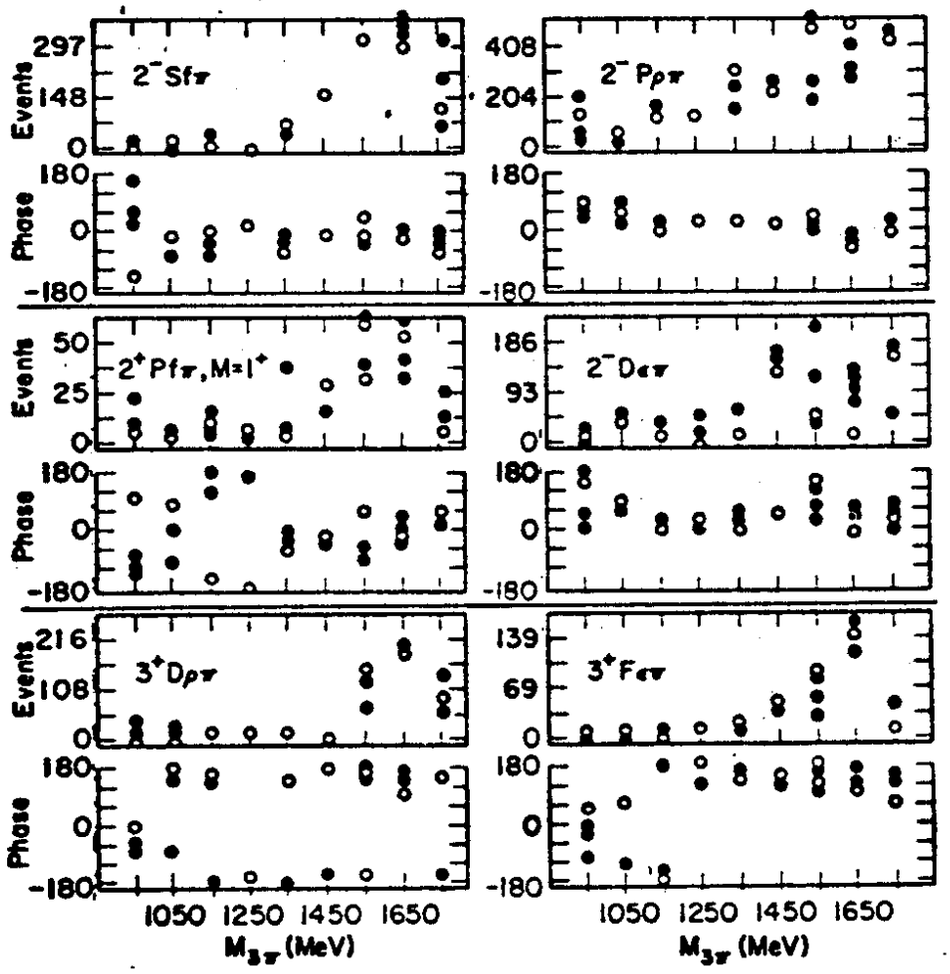
Events
Phase
297
148
0
180
0
-180
2⁻Sfπ
408
204
2⁻Pρπ
50
25
2⁺Pfπ, M=1⁺
186
93
2⁻Dεπ
216
108
3⁺Dρπ
139
69
3⁺Fεπ
1050 1250 1450 1650
M3π (MeV)

Fig. 5b

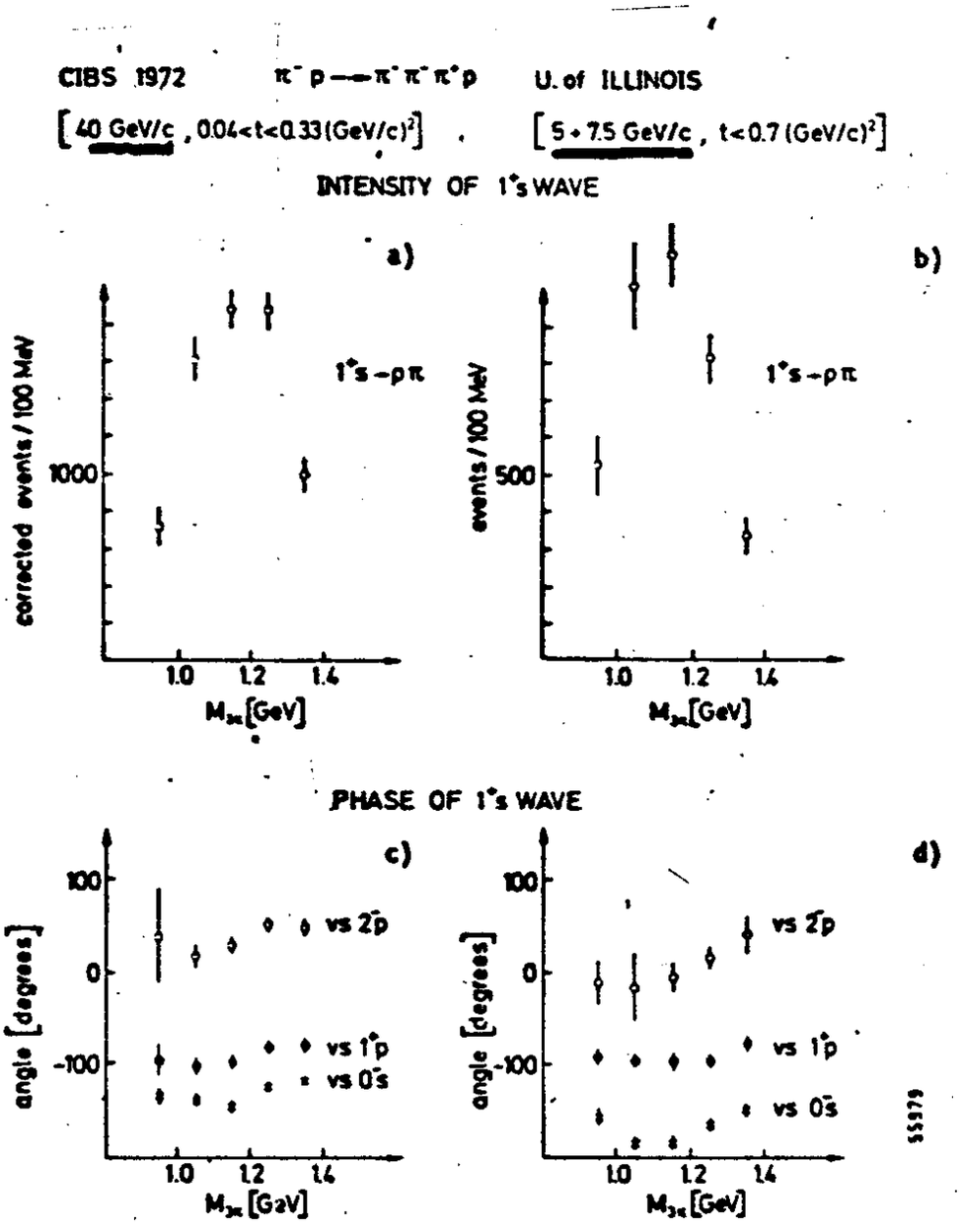
CIBS 1972 $\pi^- p \to \pi^- \pi^- \pi^+ p$ U. of ILLINOIS
[40 GeV/c, 0.04<t<0.33 (GeV/c)²] [5 ÷ 7.5 GeV/c, t<0.7 (GeV/c)²]
INTENSITY OF 1⁺s WAVE
a)
b)
corrected events / 100 MeV
events / 100 MeV
1⁺s → ρπ
1000
500
1.0
1.2
1.4
$M_{3\pi}$ [GeV]
PHASE OF 1⁺s WAVE
c)
d)
angle [degrees]
100
0
-100
vs 2⁻p
vs 1⁺p
vs 0⁻s
$M_{3\pi}$ [GeV]

Fig. 6

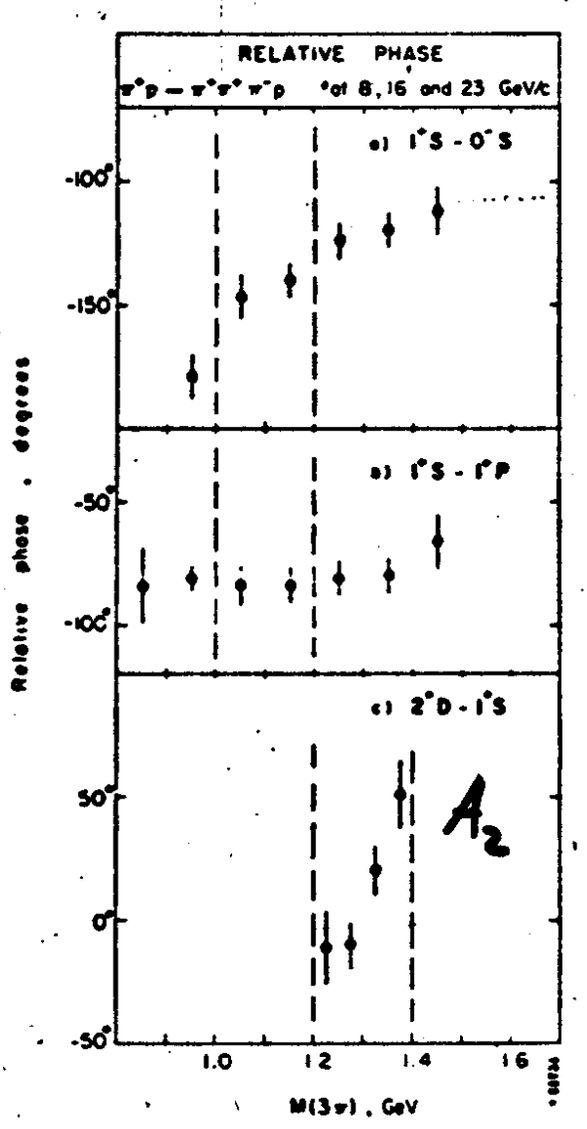
RELATIVE PHASE
π⁻p → π⁺π⁻π⁻p at 8, 16 and 23 GeV/c
a) 1⁻S - 0⁻S
b) 1⁻S - 1⁺P
c) 2⁺D - 1⁻S
A2
-100°
-150°
-50°
-100°
50°
0°
-50°
1.0
1.2
1.4
1.6
M(3π), GeV
Relative phase, degrees

Fig. 7

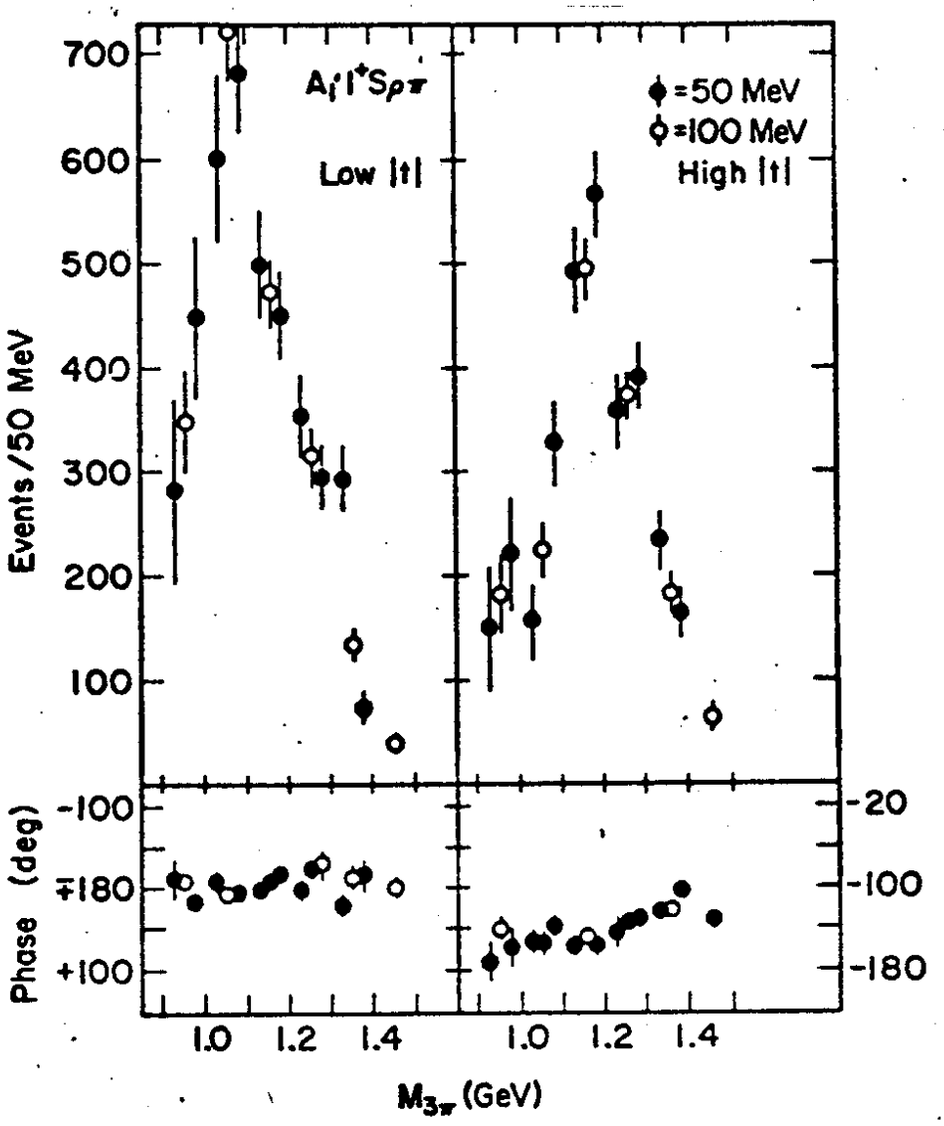
$A_1 I^G S\rho\pi$
Low |t|
High |t|
●=50 MeV
◇=100 MeV
Events/50 MeV
700
600
500
400
300
200
100
Phase (deg)
-100
±180
+100
-20
-100
-180
1.0
1.2
1.4
$M_{3\pi}$ (GeV)

Fig. 8

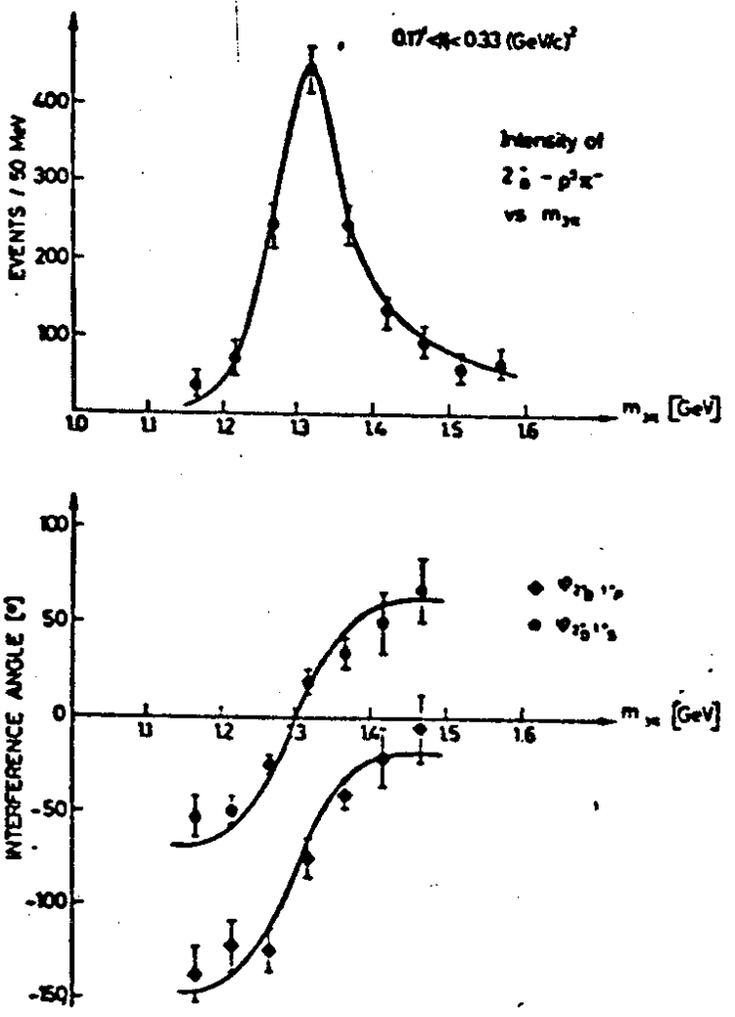

Fig. 9

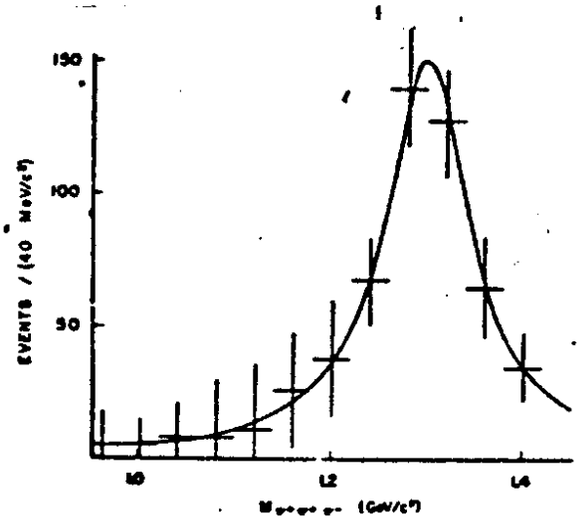

Fig. 10a

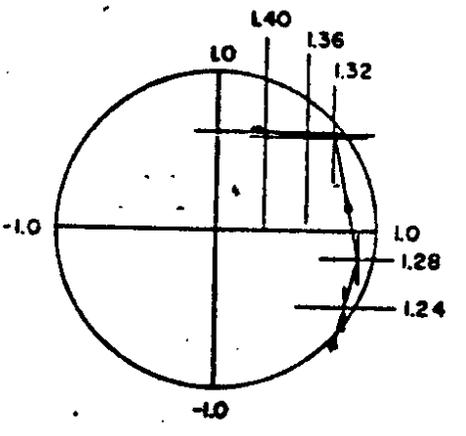

Fig. 10b

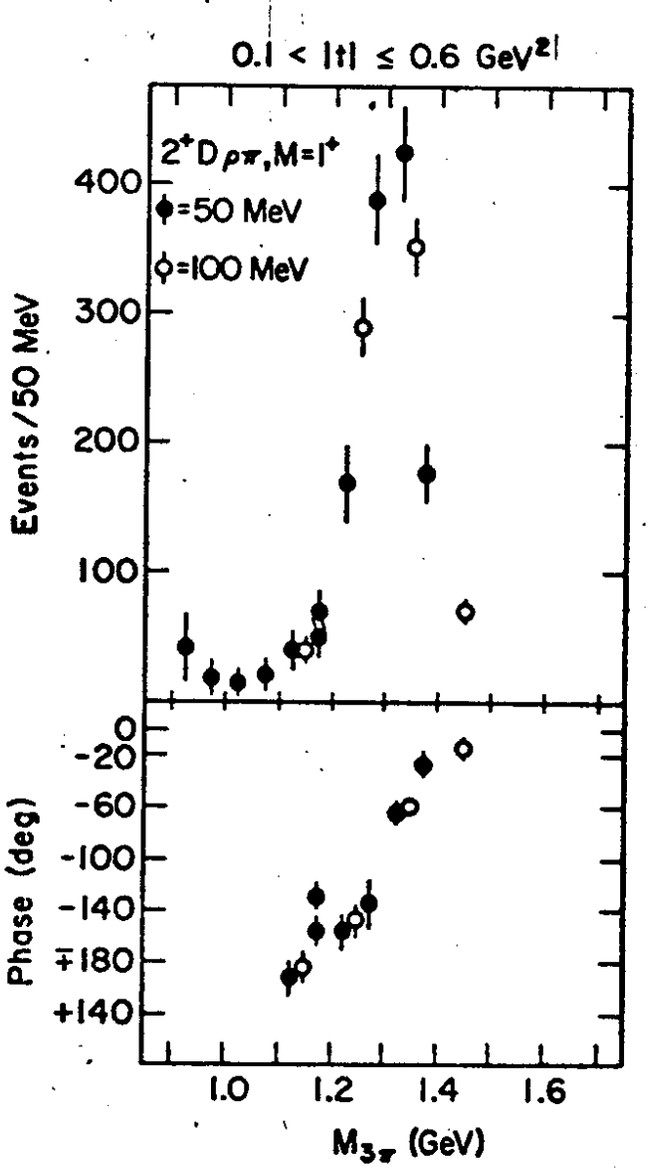
0.1 < |t| ≤ 0.6 GeV²
2⁺D ρπ, M=1⁺
●=50 MeV
◇=100 MeV
Events/50 MeV
400
300
200
100
Phase (deg)
0
-20
-60
-100
-140
±180
+140
1.0
1.2
1.4
1.6
M3π (GeV)

Fig. 11

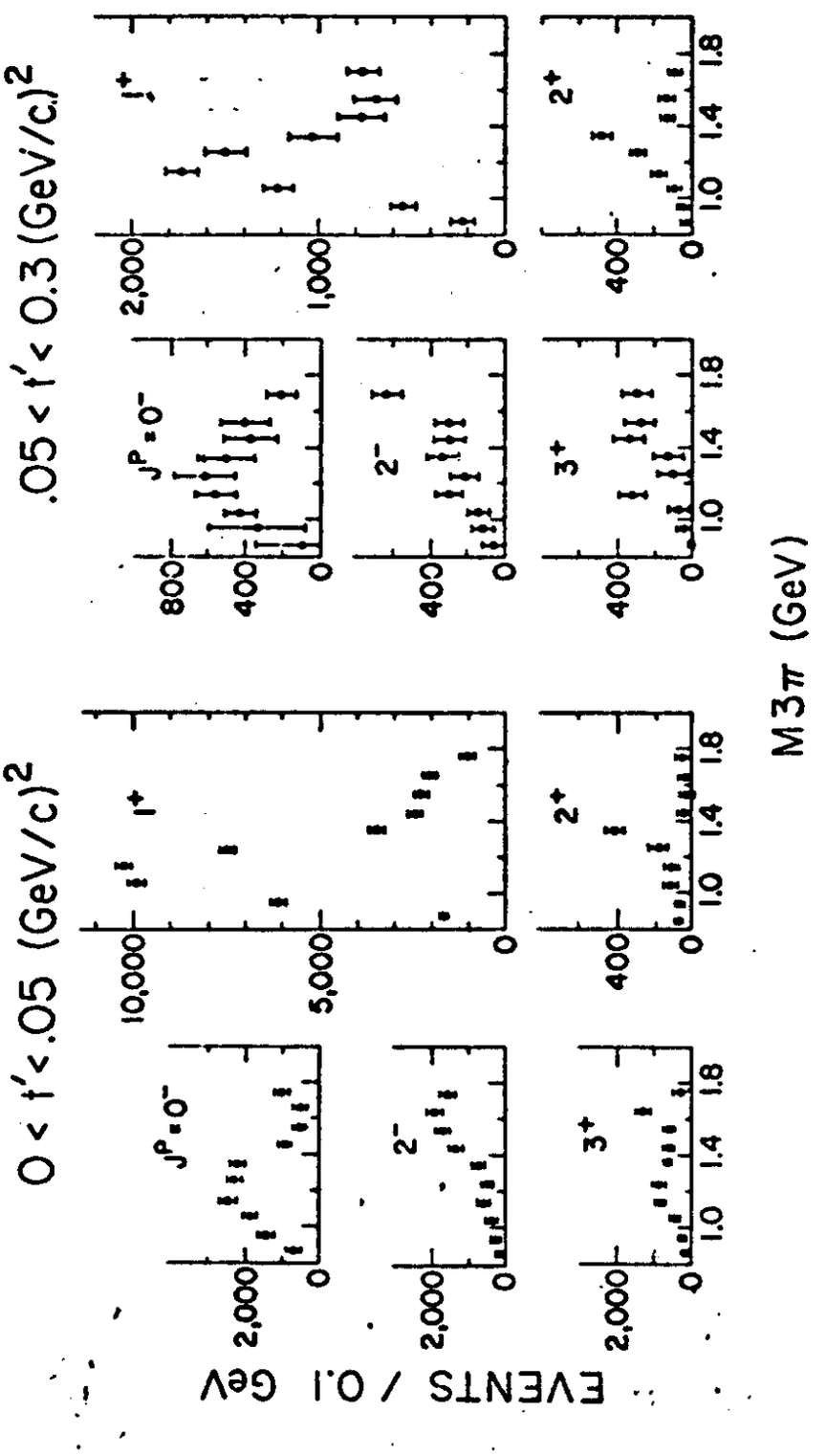

Fig. 12

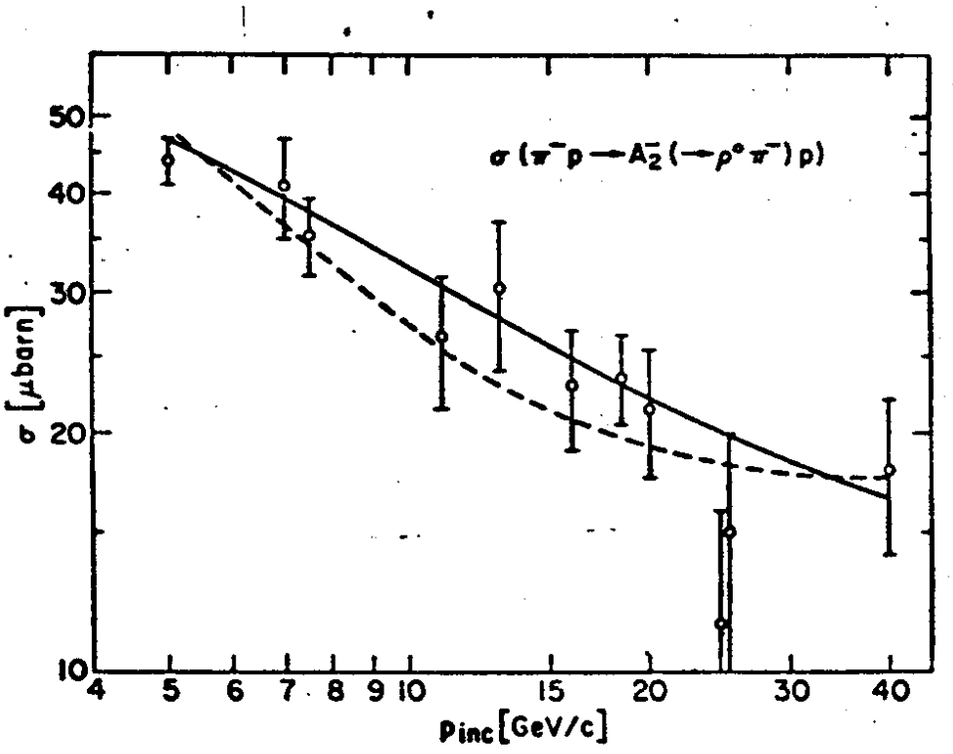

Fig. 13a

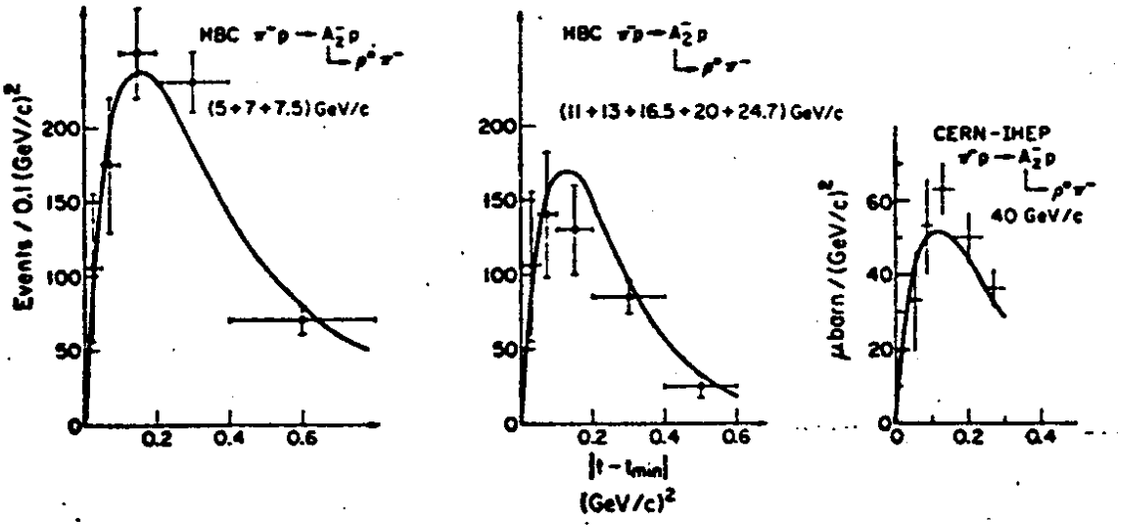

Fig. 13b

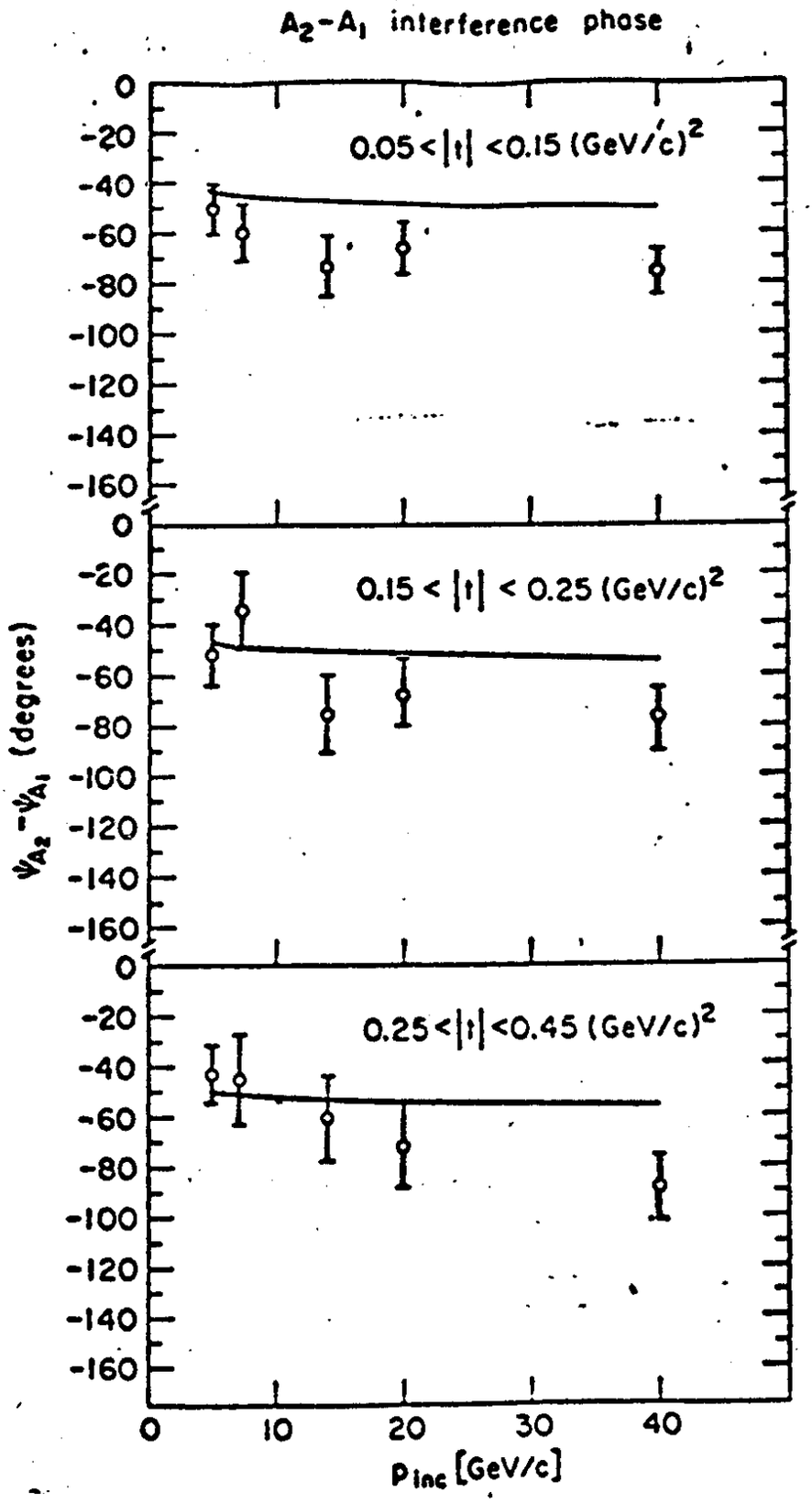
A_2-A_1 interference phase
0.05 < |t| < 0.15 (GeV/c)^2
0.15 < |t| < 0.25 (GeV/c)^2
0.25 < |t| < 0.45 (GeV/c)^2
$\psi_{A_2} - \psi_{A_1}$ (degrees)
p_{inc} [GeV/c]
0
-20
-40
-60
-80
-100
-120
-140
-160
10
20
30
40

Fig. 14

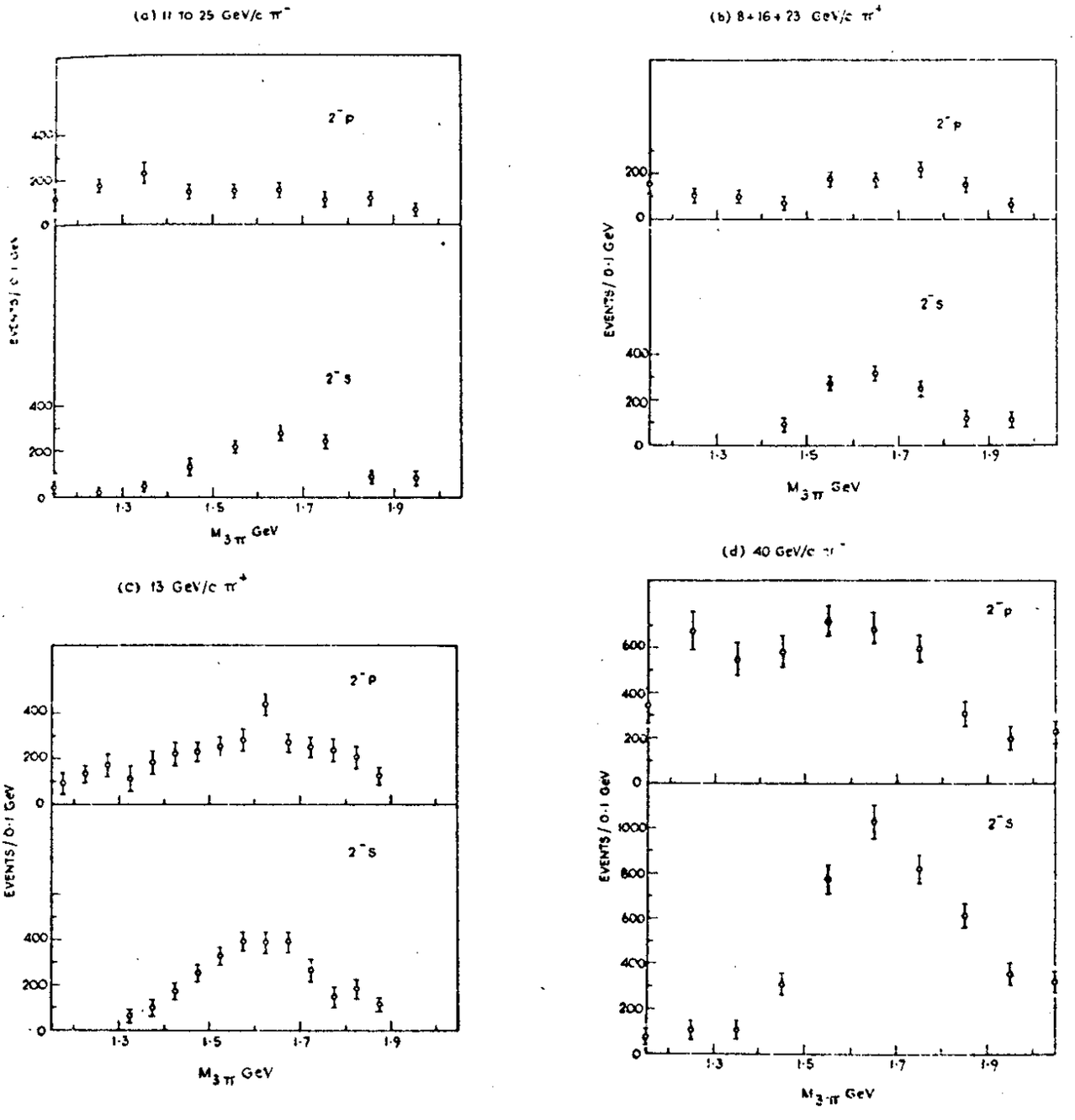
(a) 11 to 25 GeV/c π⁻
(b) 8+16+23 GeV/c π⁻
(c) 13 GeV/c π⁻
(d) 40 GeV/c π⁻
2⁻p
2⁻s
EVENTS/0·1 GeV
M3π GeV
1·3
1·5
1·7
1·9

Fig. 15

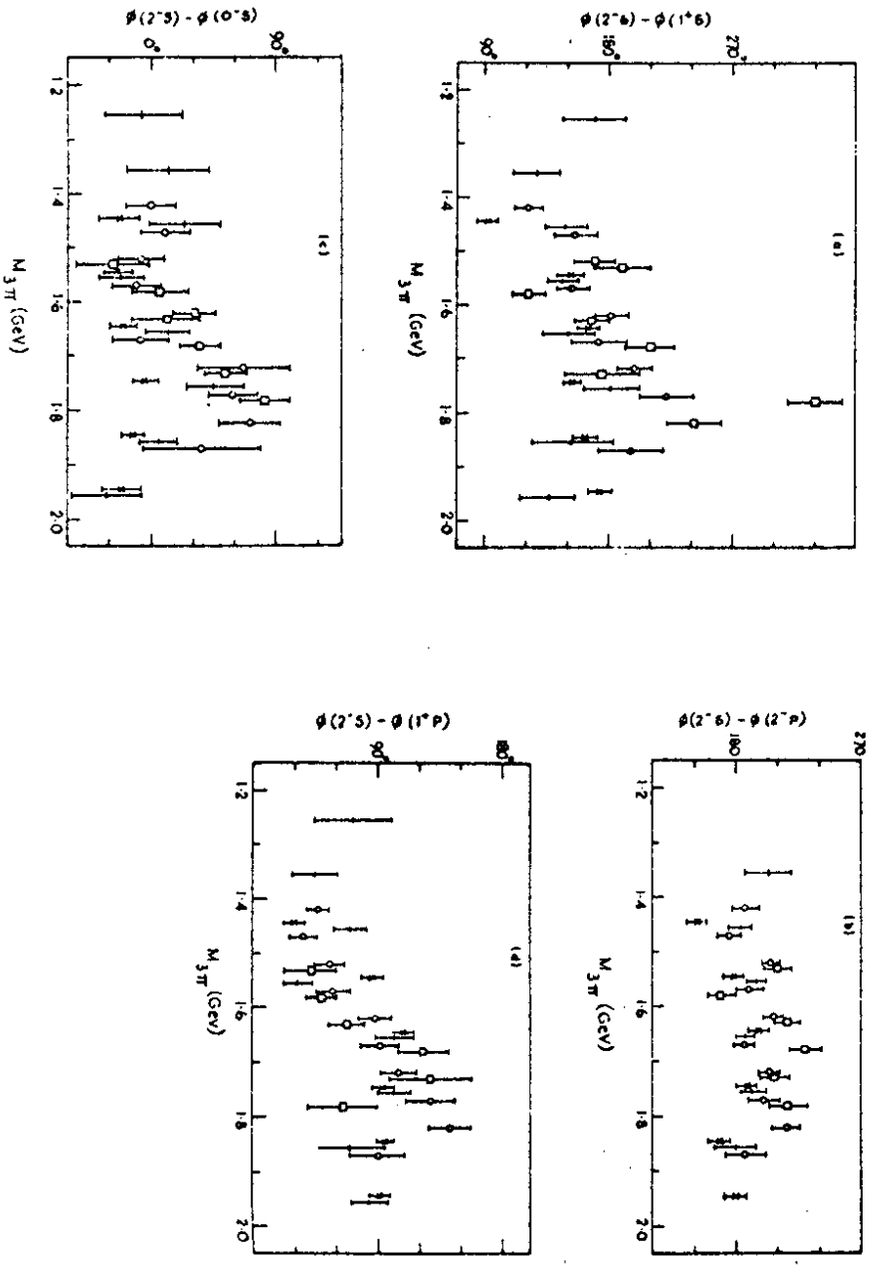

Fig. 16

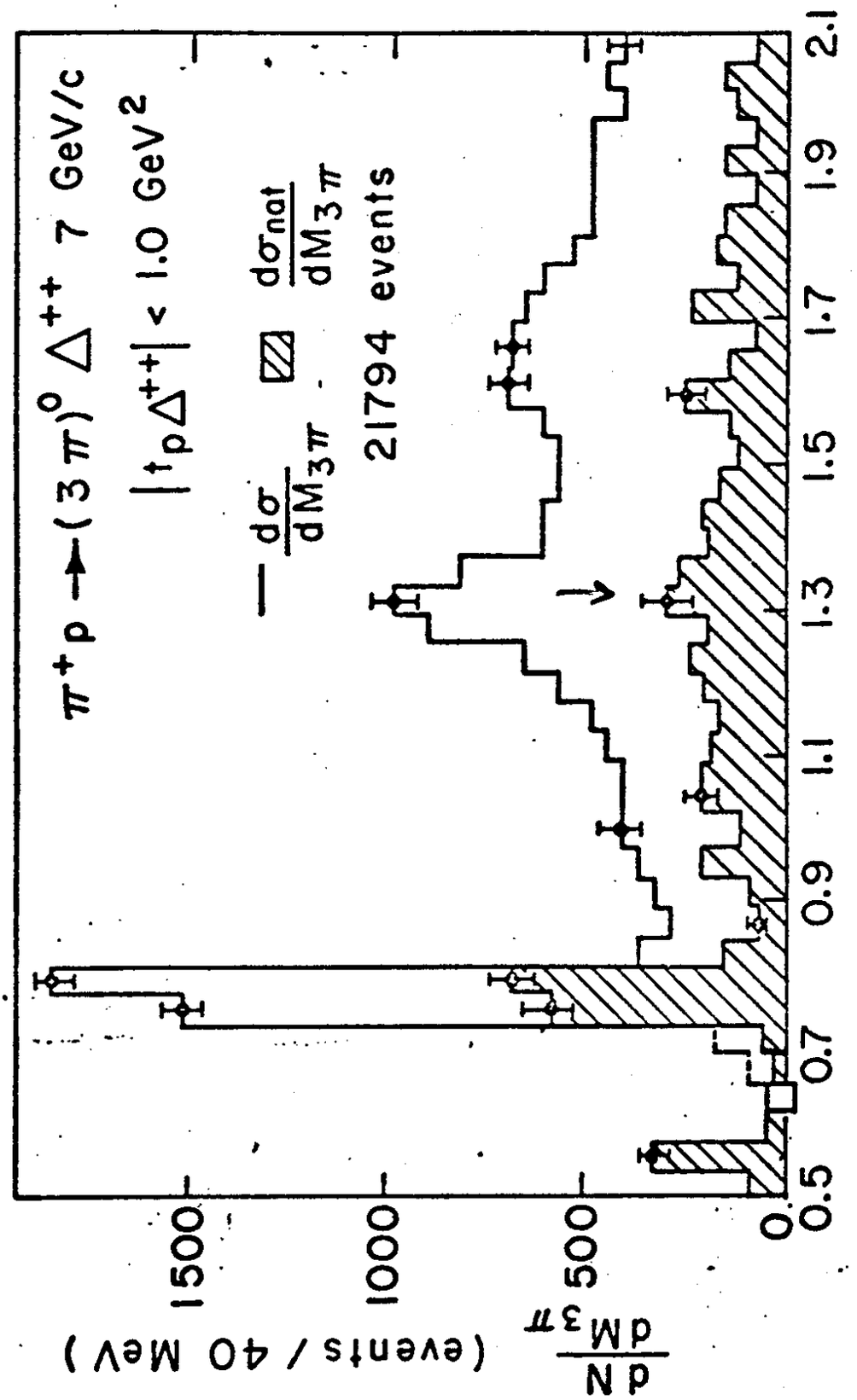
$\pi^+ p \rightarrow (3\pi)^0 \Delta^{++}$ 7 GeV/c
$|t_{p\Delta^{++}}| < 1.0$ GeV^2
$\frac{d\sigma}{dM_{3\pi}}$
$\frac{d\sigma_{nat}}{dM_{3\pi}}$
21794 events
$\frac{dN}{dM_{3\pi}}$ (events / 40 MeV)
$M_{3\pi}$
0
500
1000
1500
0.5
0.7
0.9
1.1
1.3
1.5
1.7
1.9
2.1

Fig. 17

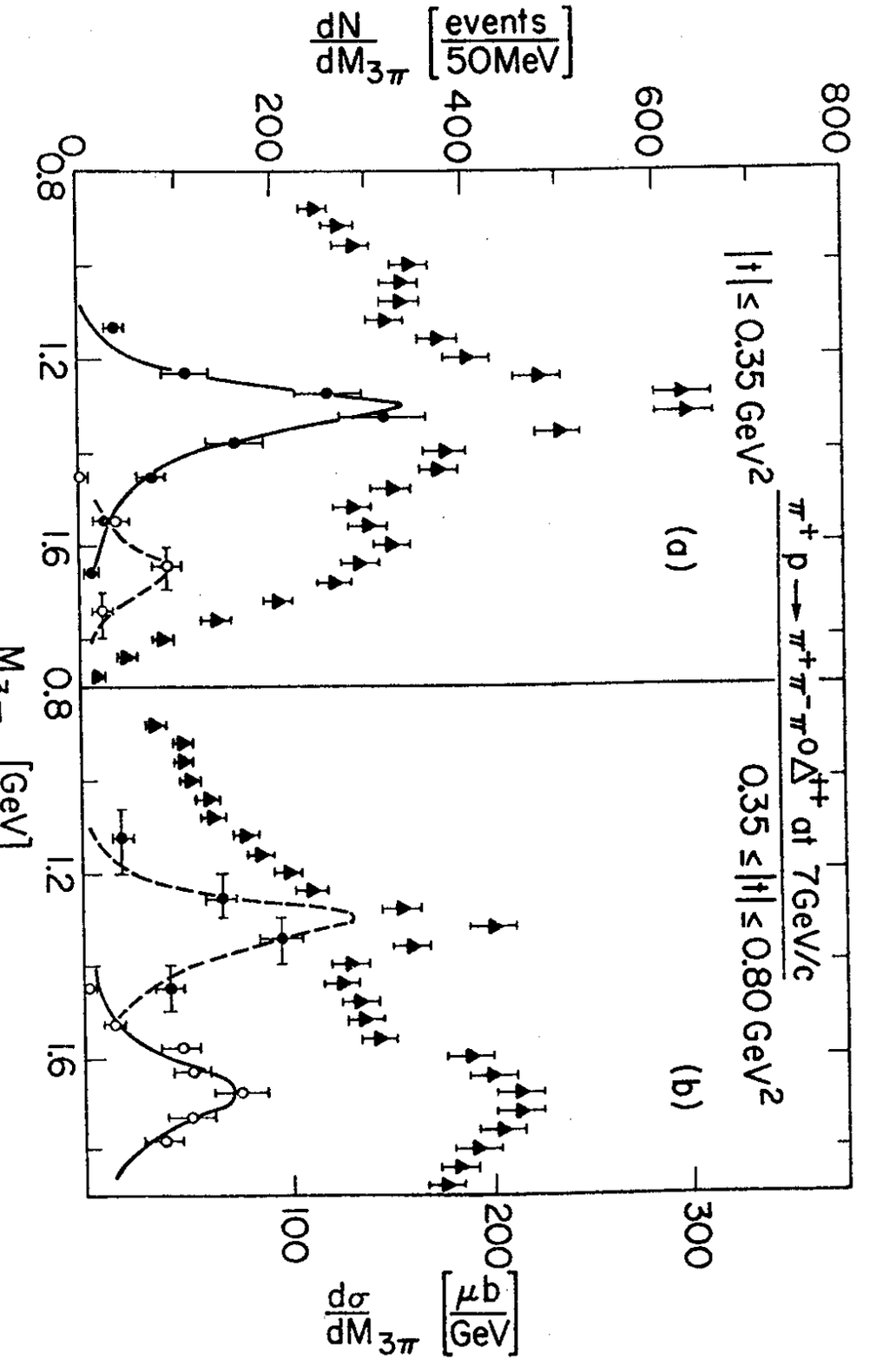
$\frac{dN}{dM_{3\pi}}$ [events / 50MeV]
$\pi^+ p \rightarrow \pi^+\pi^-\pi^0\Delta^{++}$ at 7GeV/c
$|t| \leq 0.35$ GeV^2
(a)
$0.35 \leq |t| \leq 0.80$ GeV^2
(b)
$M_{3\pi}$ [GeV]
$\frac{d\sigma}{dM_{3\pi}}$ [$\frac{\mu b}{GeV}$]

Fig. 18

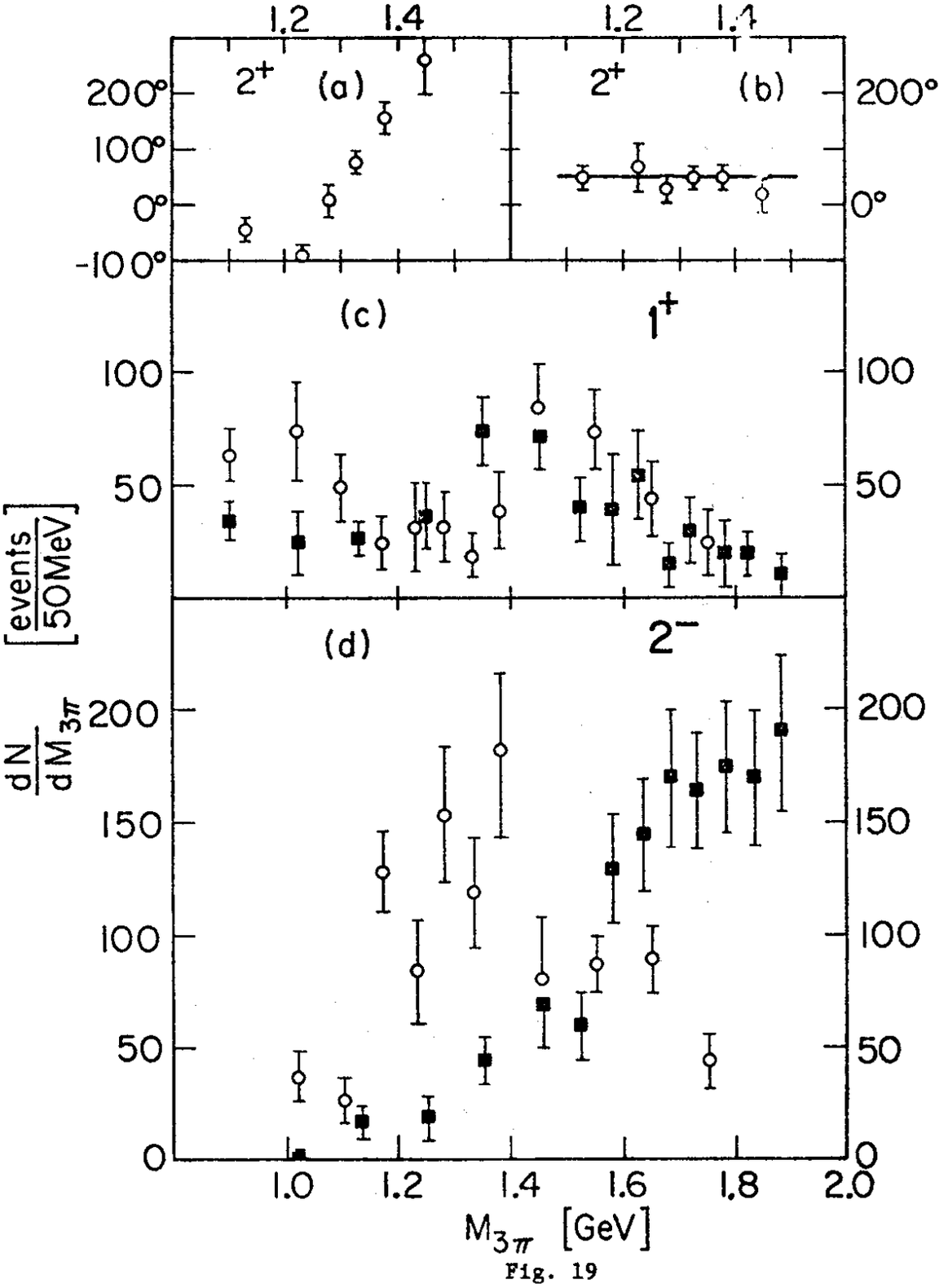
1.2
1.4
1.2
1.4
2+
(a)
2+
(b)
200°
100°
0°
-100°
200°
0°
(c)
1+
100
50
100
50
[events / 50MeV]
(d)
2−
dN/dM3π
200
150
100
50
0
200
150
100
50
0
1.0
1.2
1.4
1.6
1.8
2.0
M3π [GeV]

Fig. 19

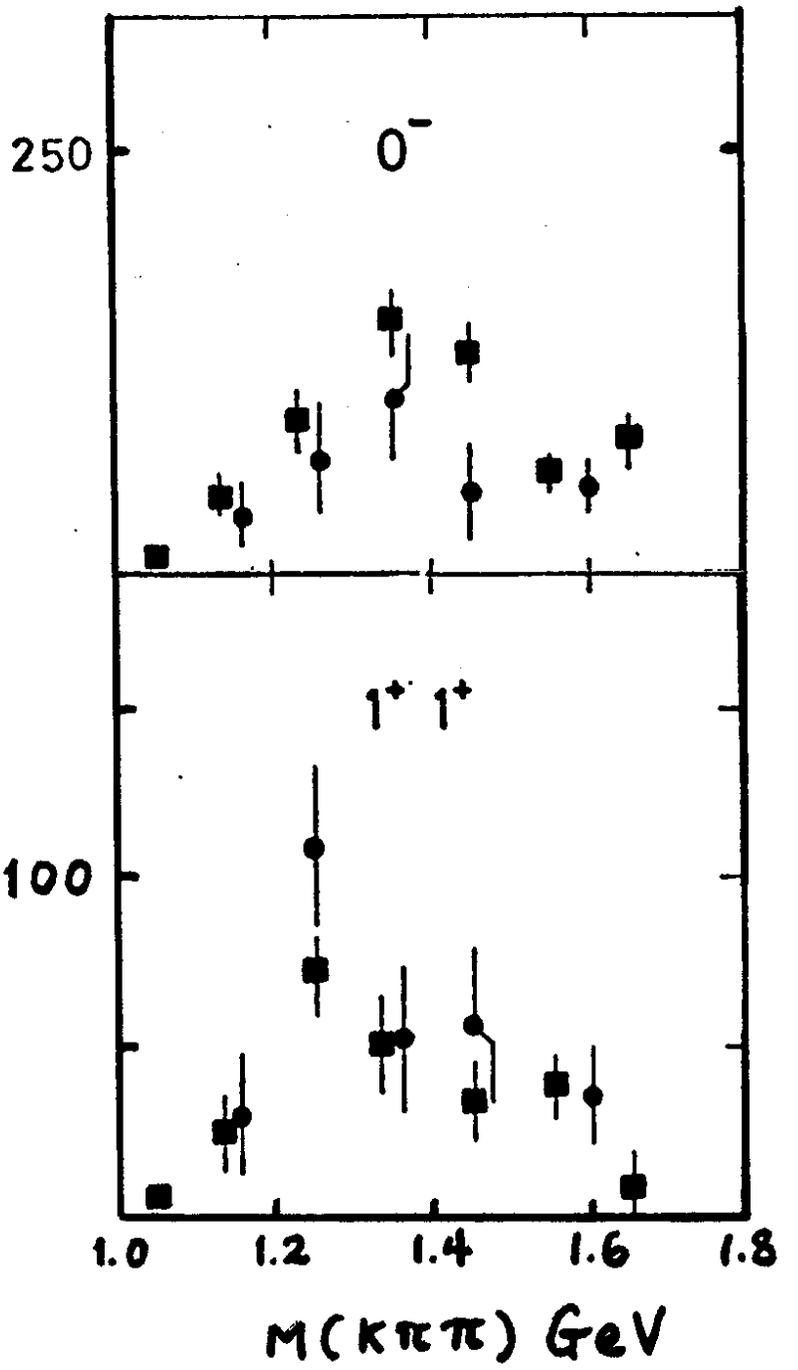

Fig. 20a

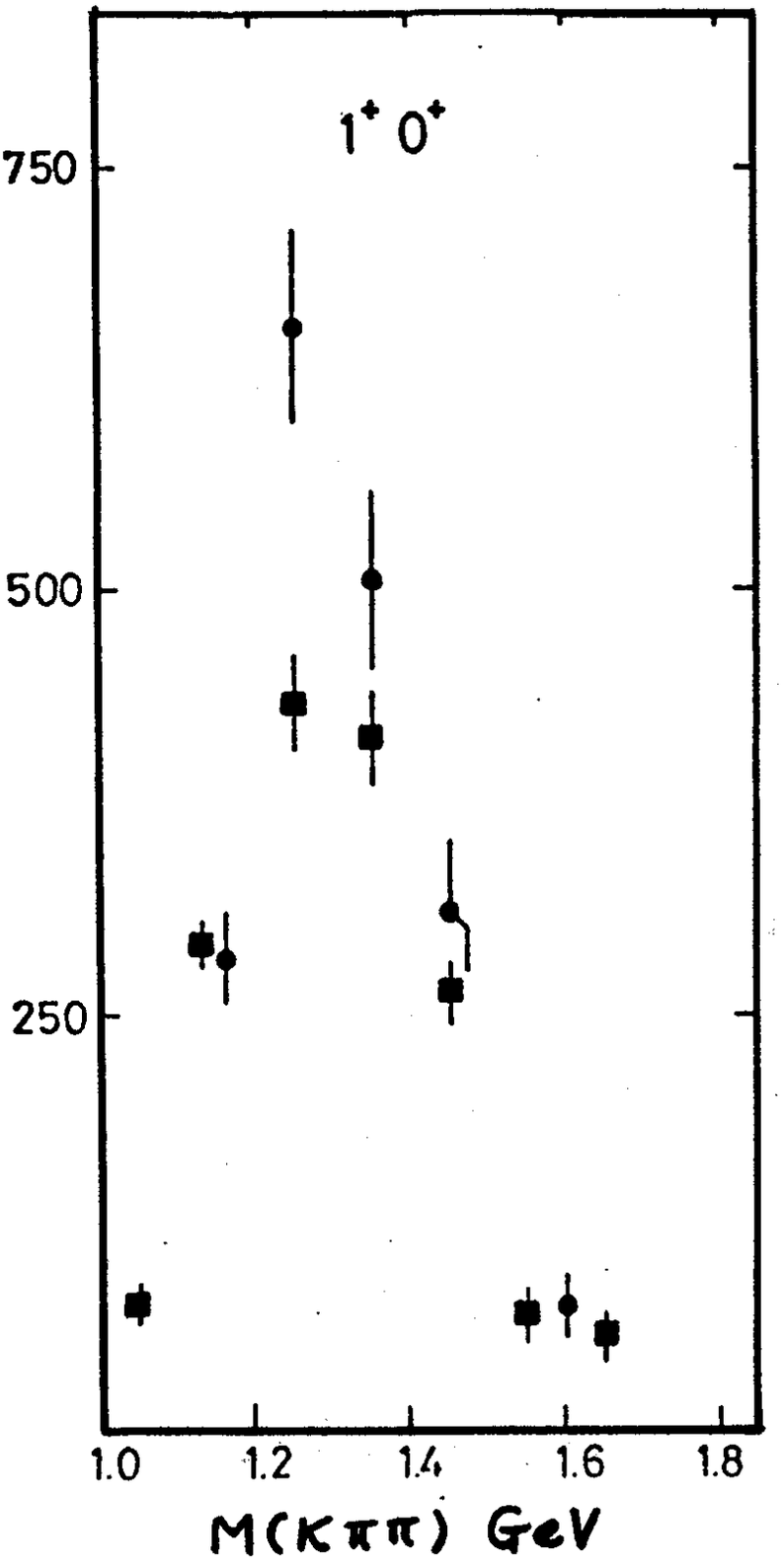

Fig. 20b

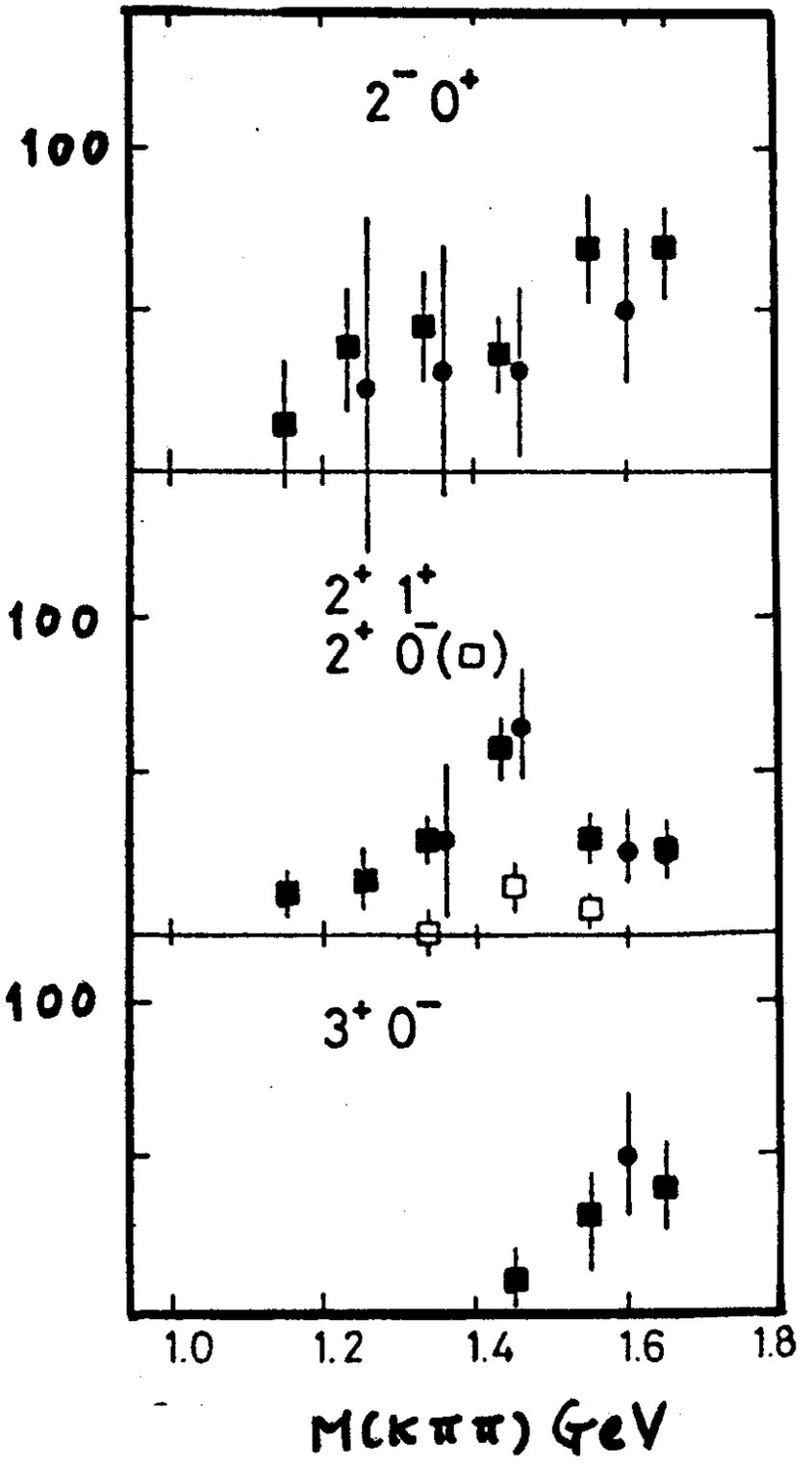

Fig. 20c

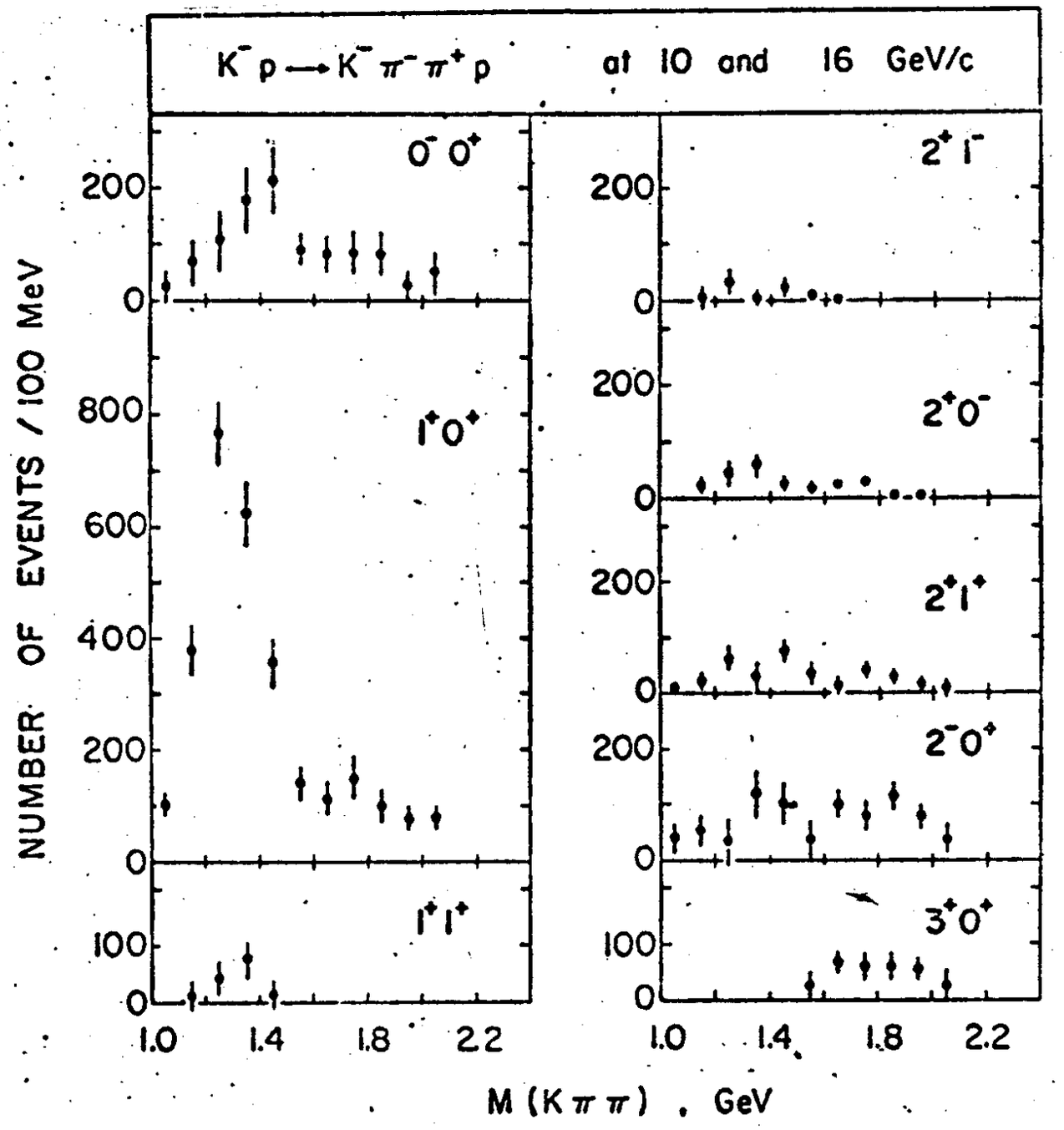
K⁻p → K⁻π⁻π⁺p at 10 and 16 GeV/c
0⁻0⁺
1⁺0⁺
1⁺1⁺
2⁺1⁻
2⁺0⁻
2⁺1⁺
2⁻0⁺
3⁺0⁺
NUMBER OF EVENTS / 100 MeV
M (Kππ) , GeV
1.0
1.4
1.8
2.2

Fig. 21

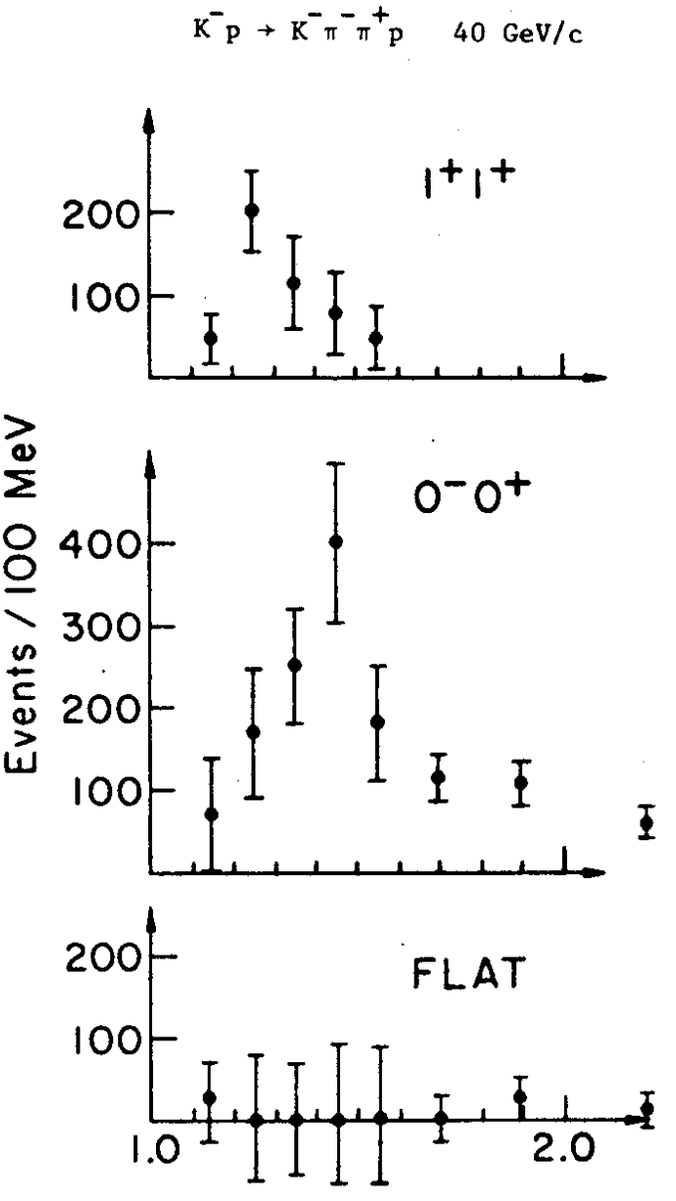
$K^-p \to K^-\pi^-\pi^+p$ 40 GeV/c
1^+1^+
0^-0^+
FLAT
Events / 100 MeV
200
100
400
300
200
100
200
100
1.0
2.0

Fig. 22a

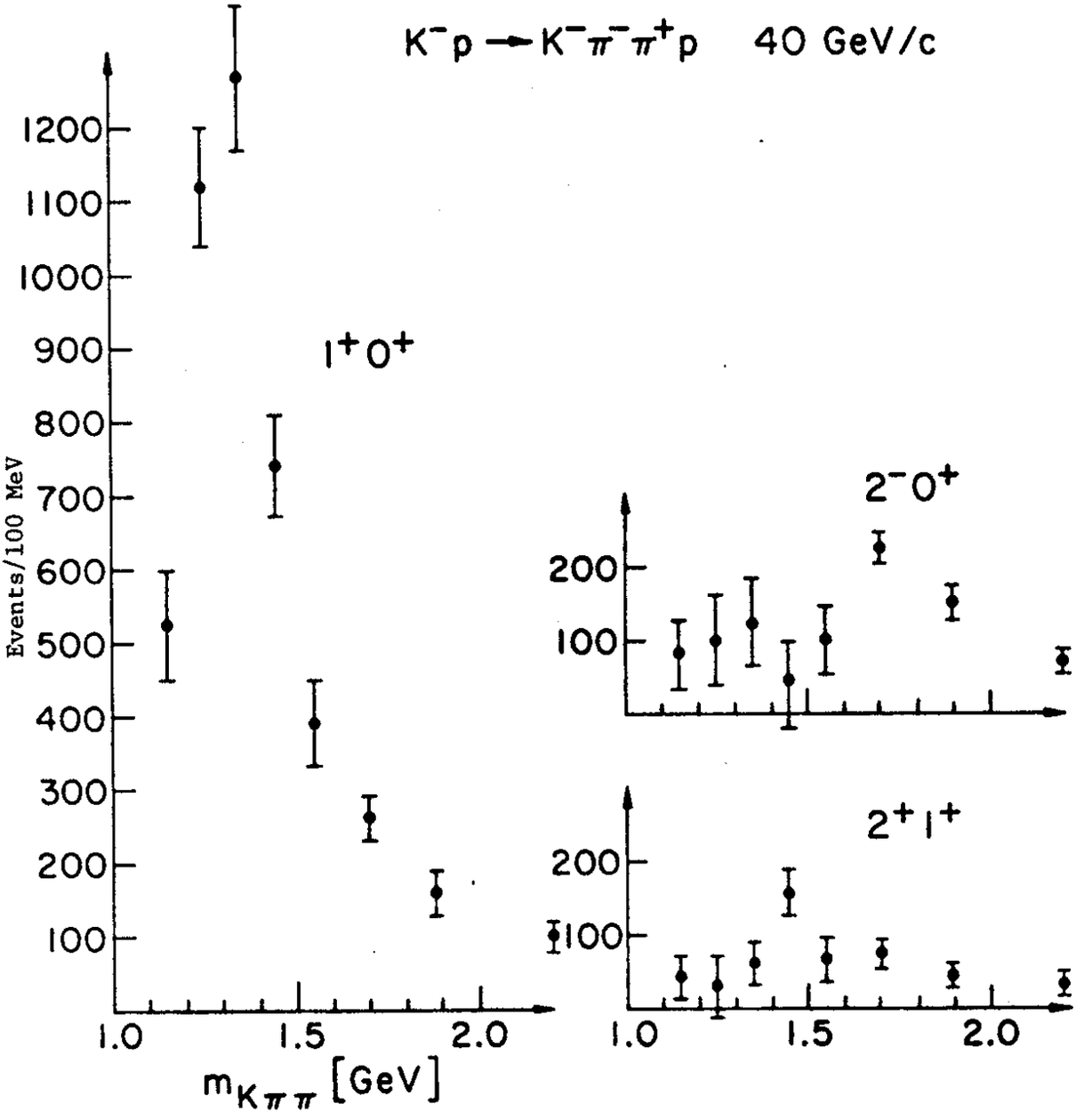
$K^-p \rightarrow K^-\pi^-\pi^+p$ 40 GeV/c
1^+0^+
2^-0^+
2^+1^+
Events/100 MeV
1200
1100
1000
900
800
700
600
500
400
300
200
100
1.0
1.5
2.0
$m_{K\pi\pi}$ [GeV]

Fig. 22b

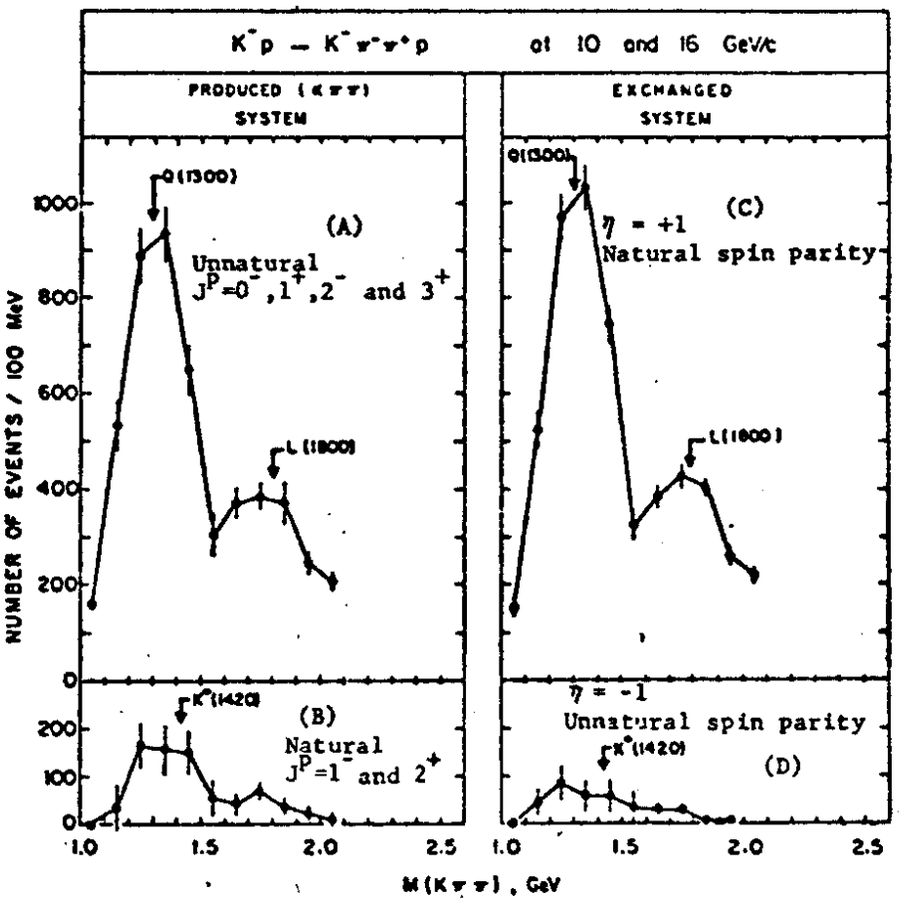
K⁻p → K⁻π⁻π⁺p at 10 and 16 GeV/c
PRODUCED (Kππ) SYSTEM
EXCHANGED SYSTEM
Q(1300)
(A)
Unnatural
J^P=0⁻,1⁺,2⁻ and 3⁺
L(1800)
(C)
η = +1
Natural spin parity
L(1800)
K*(1420)
(B)
Natural
J^P=1⁻ and 2⁺
η = -1
Unnatural spin parity
K*(1420)
(D)
NUMBER OF EVENTS / 100 MeV
M(Kππ), GeV

Fig. 23

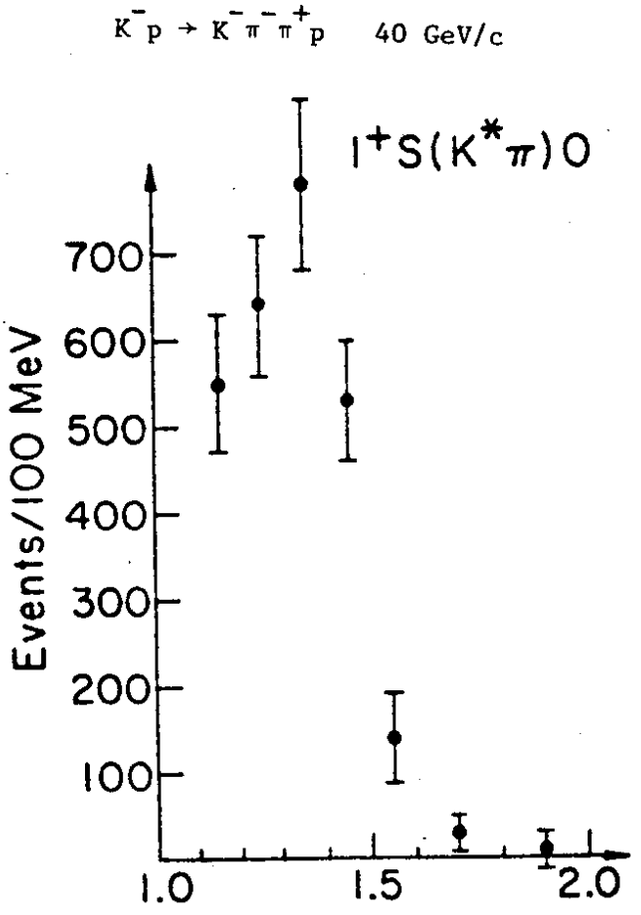
$K^-p \to K^-\pi^-\pi^+p$ 40 GeV/c
$I^+S(K^*\pi)0$
Events/100 MeV
700
600
500
400
300
200
100
1.0
1.5
2.0

Fig. 24a

$K^- p \rightarrow K^- \pi^- \pi^+ p$ 40 GeV/c

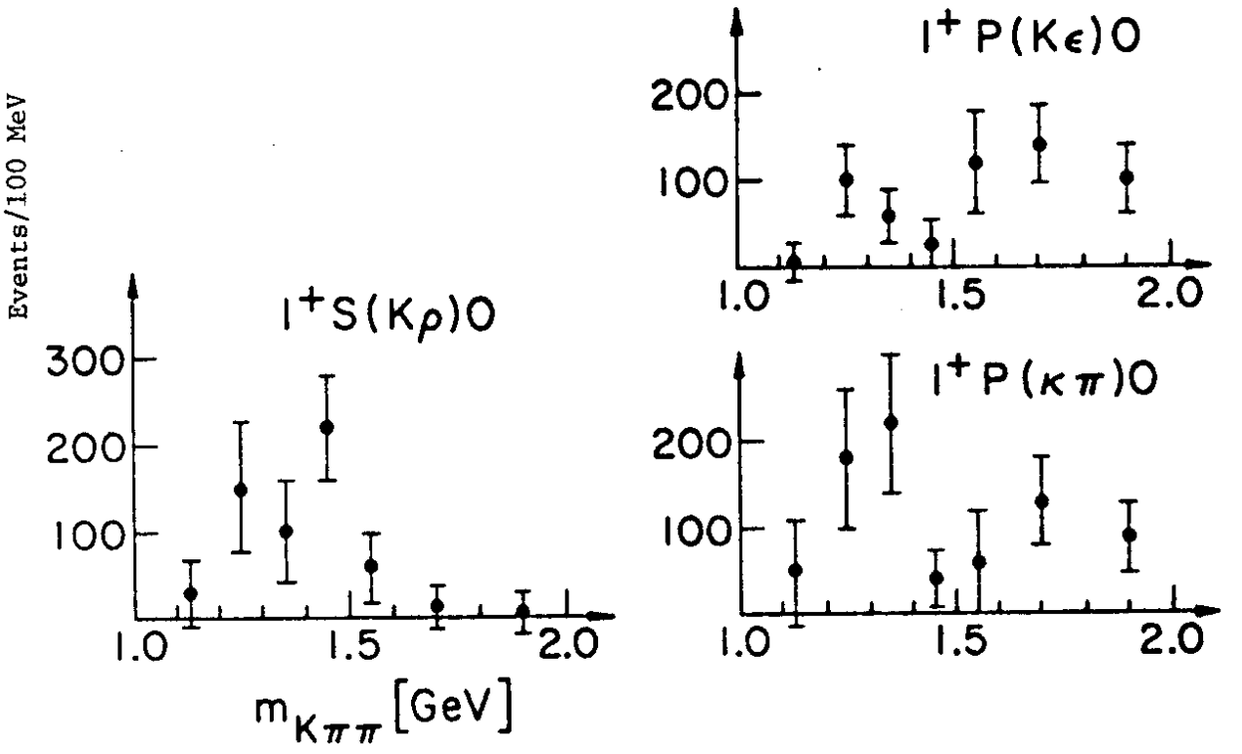

Fig. 24b

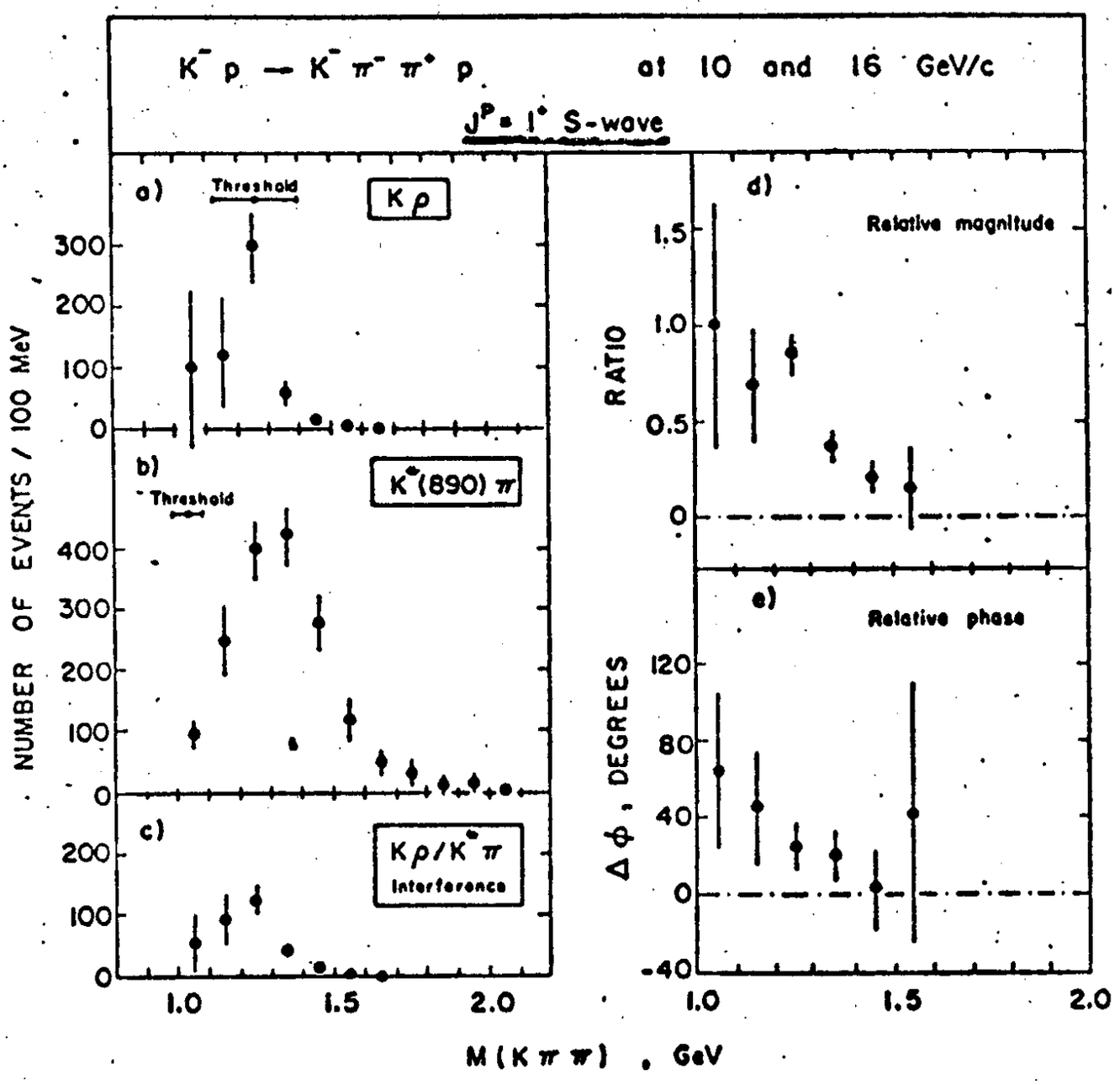
K⁻ p → K⁻ π⁻ π⁺ p at 10 and 16 GeV/c
J^P = 1^+ S-wave
a)
Threshold
Kρ
b)
Threshold
K*(890) π
c)
Kρ/K*π
Interference
d)
Relative magnitude
RATIO
e)
Relative phase
Δφ, DEGREES
NUMBER OF EVENTS / 100 MeV
M(K π π), GeV

Fig. 25

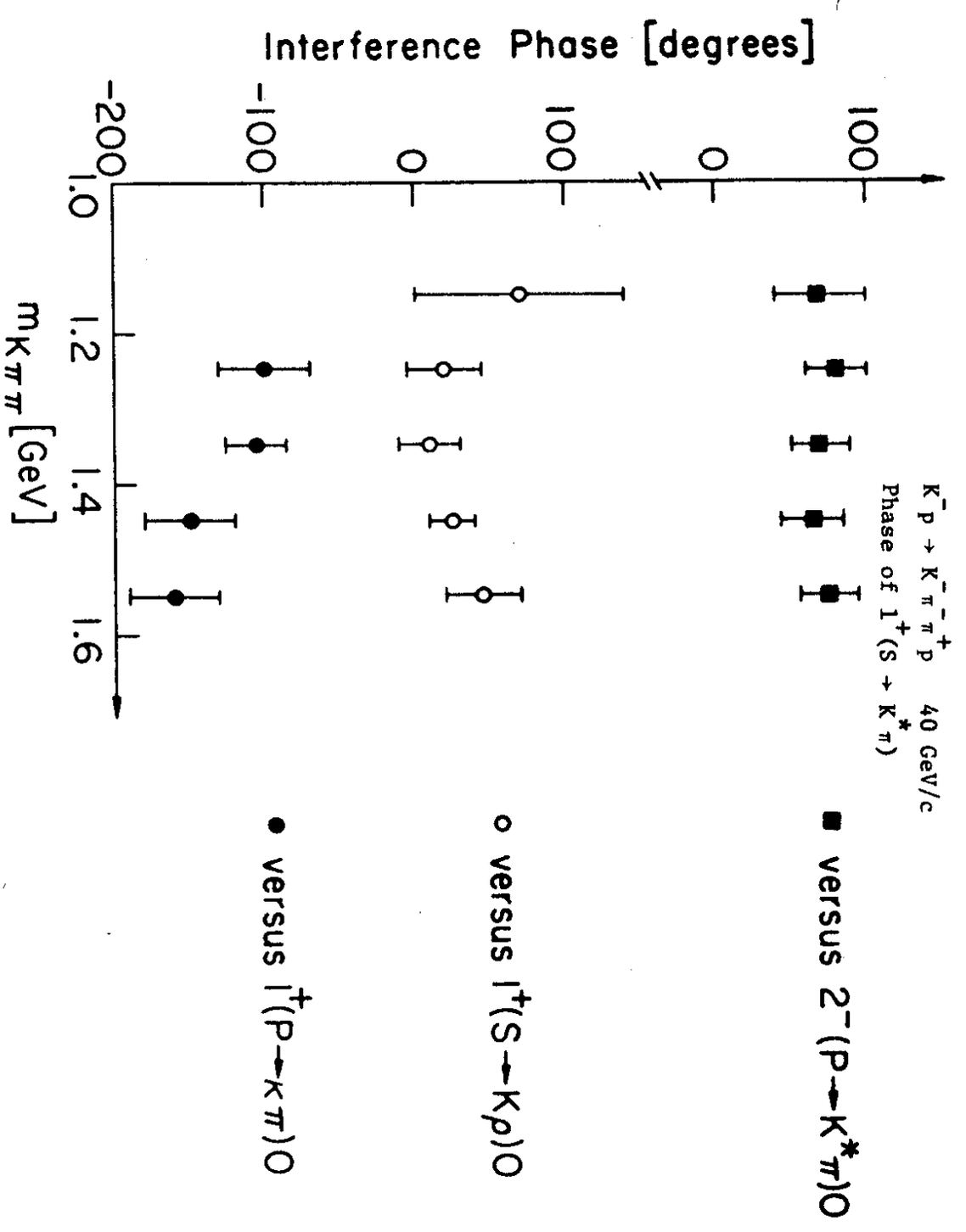
Interference Phase [degrees]
-200
-100
0
100
0
100
1.0
1.2
1.4
1.6
$m_{K\pi\pi}$ [GeV]
$K^- p \to K^- \pi^- \pi^+ p$ 40 GeV/c
Phase of $1^+(S \to K^*\pi)$
■ versus $2^-(P \to K^*\pi)0$
o versus $1^+(S \to K\rho)0$
● versus $1^+(P \to K\pi)0$

Fig. 26

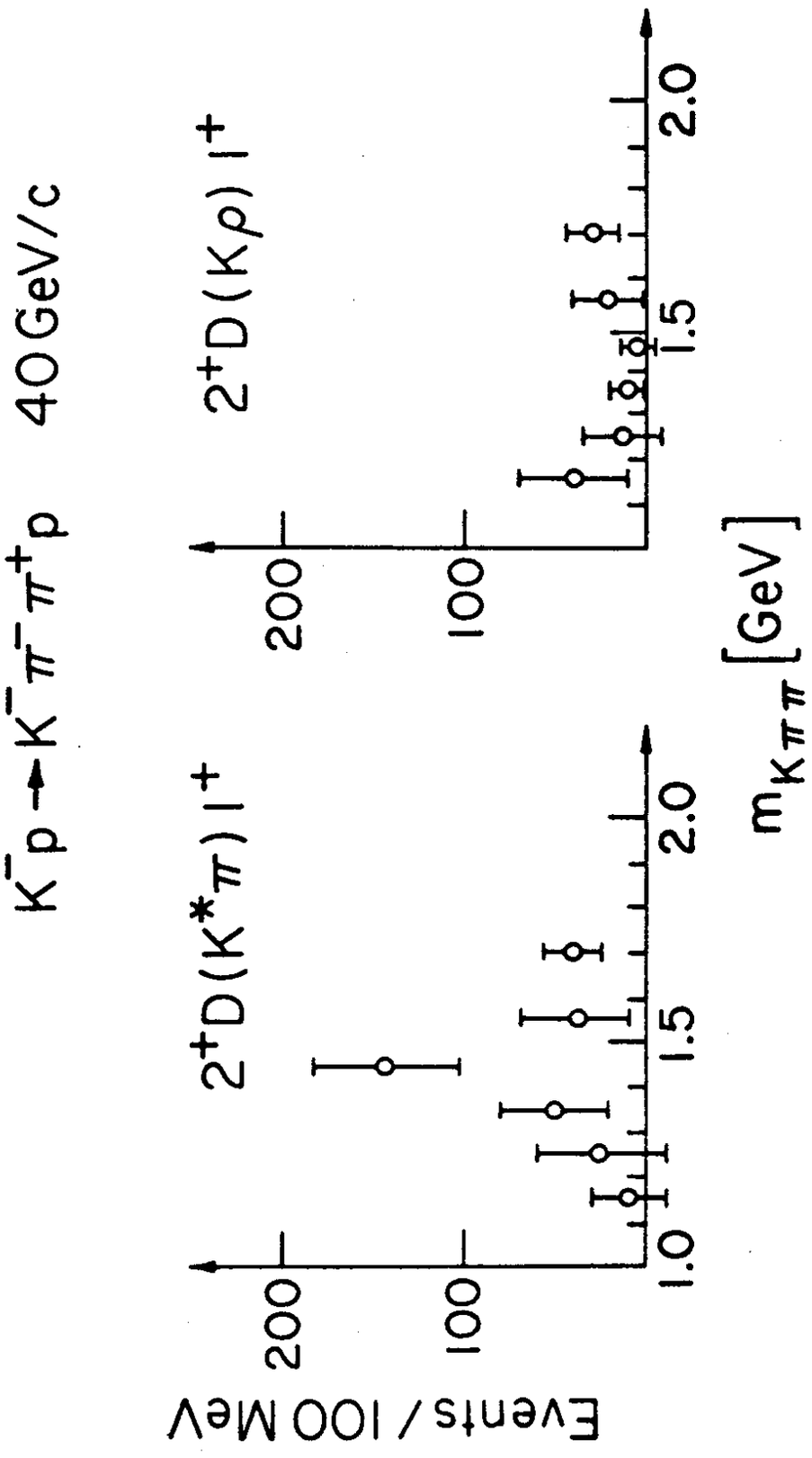
$K^-p \to K^-\pi^-\pi^+p$ 40 GeV/c
$2^+D(K^*\pi)I^+$
$2^+D(K\rho)I^+$
Events / 100 MeV
200
100
1.0
1.5
2.0
$m_{K\pi\pi}$ [GeV]

Fig. 27

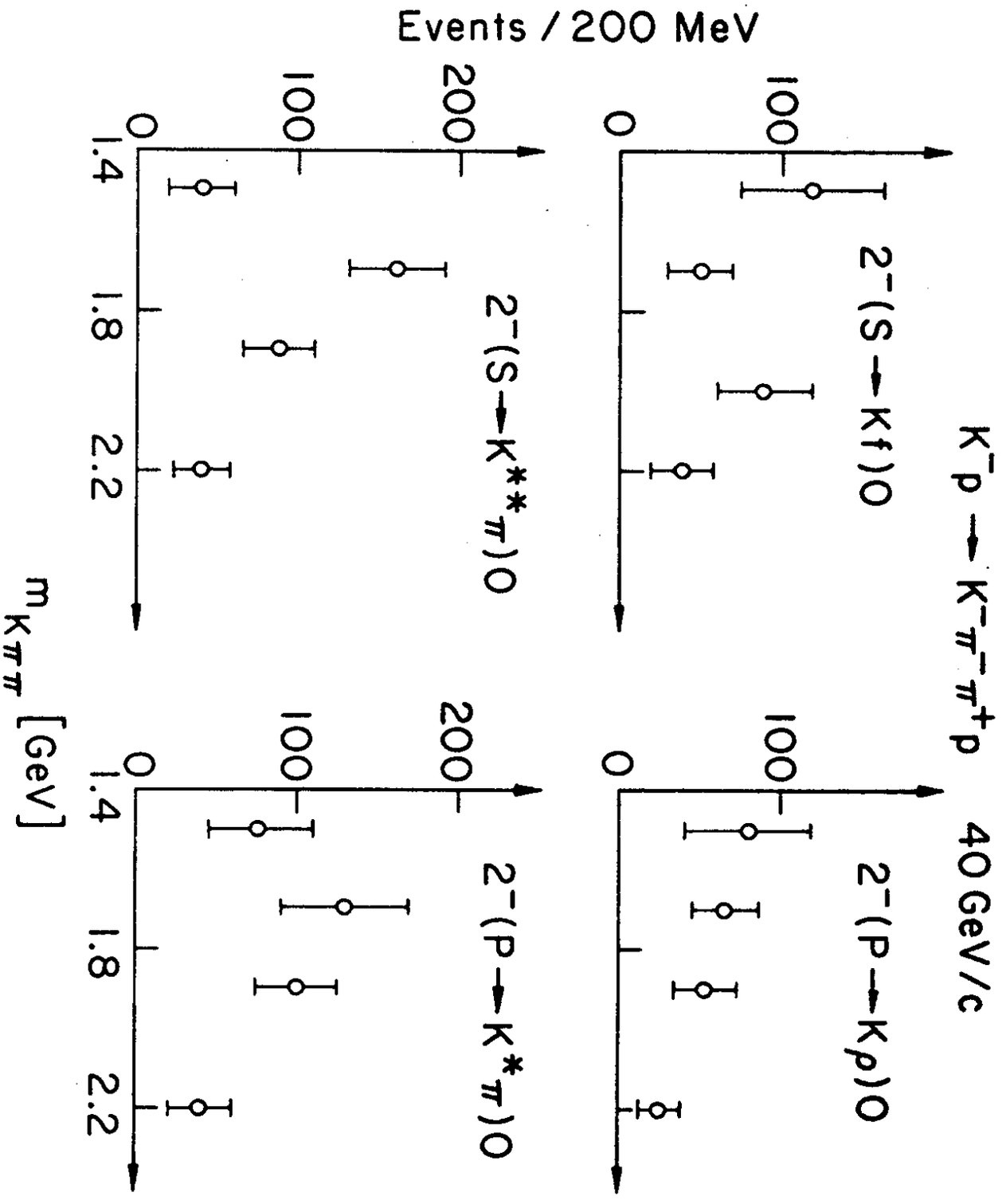
Events / 200 MeV
$K^-p \rightarrow K^-\pi^-\pi^+p$ 40 GeV/c
$2^-(S \rightarrow Kf)0$
$2^-(S \rightarrow K^{**}\pi)0$
$2^-(P \rightarrow K\rho)0$
$2^-(P \rightarrow K^*\pi)0$
$m_{K\pi\pi}$ [GeV]
0
100
200
1.4
1.8
2.2

Fig. 28

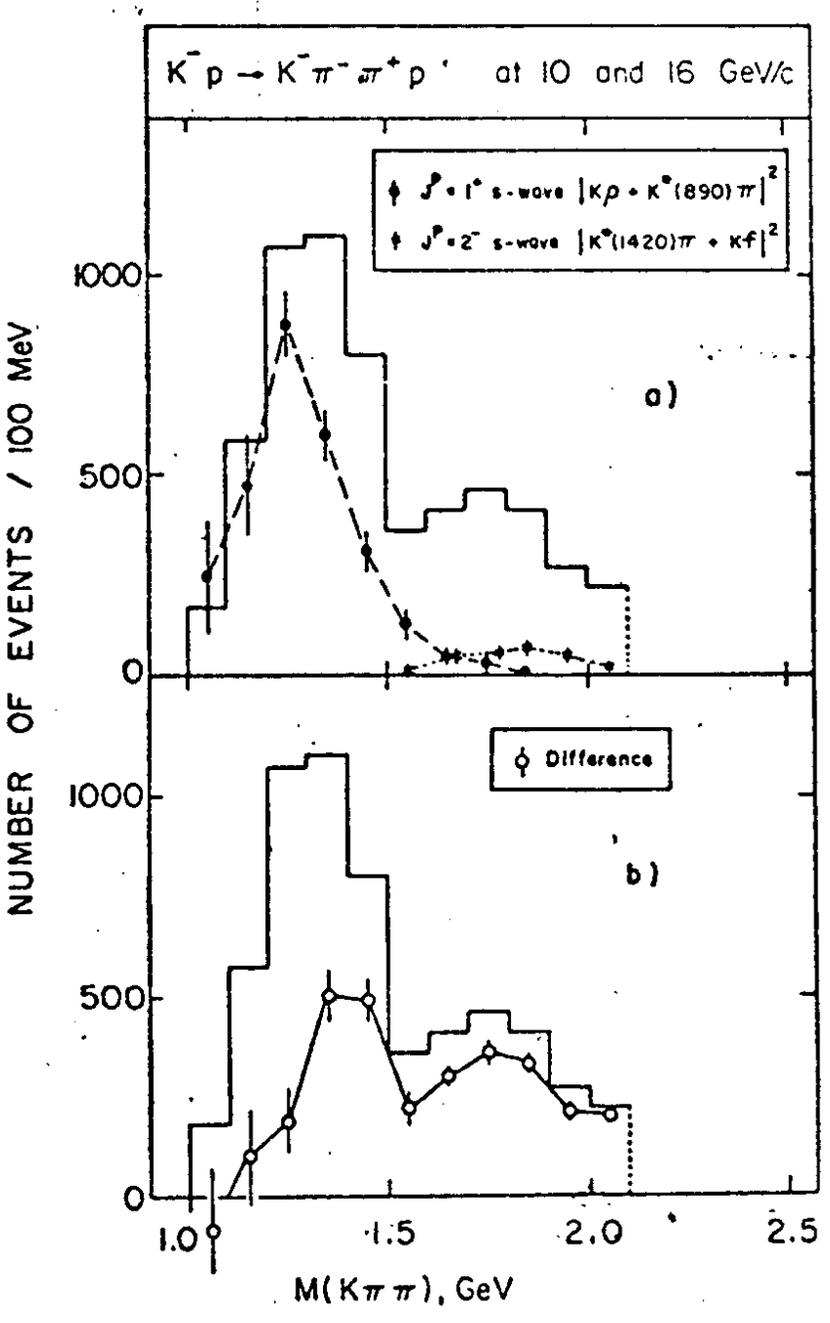
$K^- p \to K^- \pi^- \pi^+ p$ ' at 10 and 16 GeV/c
$J^P = 1^+$ s-wave $|K\rho + K^*(890)\pi|^2$
$J^P = 2^-$ s-wave $|K^*(1420)\pi + Kf|^2$
a)
Difference
b)
NUMBER OF EVENTS / 100 MeV
1000
500
0
1.0
1.5
2.0
2.5
M(Kππ), GeV

Fig. 29